Surface Analysis of Lipids by Mass Spectrometry: More than Just Imaging.

Shane R. Ellis[a], Simon H. Brown[c] Marc in het Panhuis[b], Stephen J. Blanksby[a], Todd W. Mitchell[c]*

[a]ARC Centre of Excellence for Free Radical Chemistry and Biotechnology, School of Chemistry, University of Wollongong, Wollongong, NSW 2522, Australia

[b]Soft Materials Group, School of Chemistry and Intelligent Polymer Research Institute, ARC Centre of Excellence for Electromaterials Science, University of Wollongong, Wollongong, NSW 2522, Australia

[c]School of Health Sciences, University of Wollongong, Wollongong, NSW 2522, Australia

*Corresponding author: toddm@uow.edu.au

Keywords: Lipidomics, ambient ionization, mass spectrometry imaging, thin-layer chromatography

Abstract

Mass spectrometry is now an indispensable tool for lipid analysis and is arguably the driving force in the renaissance of lipid research. In its various forms, mass spectrometry is uniquely capable of resolving the extensive compositional and structural diversity of lipids in biological systems. Furthermore, it provides the ability to accurately quantify molecular-level changes in lipid populations associated with changes in metabolism and environment; bringing lipid science to the "omics" age. The recent explosion of mass spectrometry-based surface analysis techniques is fuelling further expansion of the lipidomics field. This is evidenced by the numerous papers published on the subject of mass spectrometric imaging of lipids in recent years. While imaging mass spectrometry provides new and exciting possibilities, it is but one of the many opportunities direct surface analysis offers the lipid researcher. In this review we describe the current state-of-the-art in the direct surface analysis of lipids with a focus on tissue sections, intact cells and thin-layer chromatography substrates. The suitability of these different approaches towards analysis of the major lipid classes along with their current and potential applications in the field of lipid analysis are evaluated.

Abbreviations: 2-AEP, 2-aminophosphonolipid; 9-AA, 9-aminoacridine; APCI, atmospheric pressure chemical ionization; AP-MALDI, atmospheric pressure matrix-assisted laser desorption ionization; ASAP, atmospheric pressure solids analysis probe; Cer, ceramide; Cer1P, ceramide-1-phosphate; CHCA, α-cyano-4-hydroxycinnamic acid; CID, collision-induced dissociation; DAG, diacylglyceride; DAN, 1,5-diaminonapthalene; DAPPI, desorption atmospheric pressure photoionization; DART, direct analysis in real time; DESI, desorption electrospray ionization; DHA, 2,6-dihydroxyacetphenone; DHB, 2,5-dihydroxybenzoic acid; DIOS, desorption/ionisation from porous silicon; DMAN, 1,8-bis(dimethylamino)naphthalene; EASI, easy ambient sonic spray ionization; ELDI, electrospray laser desorption ionization; ESI, electrospray ionization; FAEE, fatty acid ethyl ester; FAME, fatty acid methyl ester; FFA, free fatty acid; GalCer, galactosylceramide; GALDI, graphite-assisted laser desorption ionization; GL, ganglioside; GSL, glycosphingolipid; IR, infrared; IR-MALDI, infrared matrix-assisted laser desorption ionization; LacCer, lactosylceramide; LAESI, laser ablation electrospray ionization, LDI, laser desorption ionization; LESA, liquid extraction surface analysis; LIAD, laser-induced acoustic desorption; LPE, lyso phosphatidylethanolamine; LPS, lyso phosphatidylserine; LTP, low temperature plasma; MALDESI, matrix-assisted laser desorption electrospray ionization; MALDI, matrix-assisted laser desorption ionization; MBT, 2-mercaptobenzothiazole; ME-SIMS, matrix-enhanced secondary ion mass spectrometry; Met-SIMS, metal-assisted secondary ion mass spectrometry; MS/MS, tandem mass spectrometry; MTPFPP, meso-tetrakis (pentaflurophenyl) porphyrin; NALDI, nanowire-assisted laser desorption ionization; NIMS, nanostructure-initiator mass spectrometry; PA, phosphatidic acid; PC, phosphatidylcholine; PCA, principal component analysis; PE, phosphatidylethanolamine; PESI, probe electrospray ionization PG, phosphatidylglycerol; PI, phosphatidylinositol; PL, phospholipid; PMMA, poly(methyl methacrylate); PNA, p-nitroaniline; PS, phosphatidylserine; PSI, paper spray ionization; PTFE, polytetrafluoroethylene; PVDF, polyvinylidene difluoride; REIMS, rapid evaporative ionization mass spectrometry; SIMS, secondary ion mass spectrometry; SM, sphingomyelin; SSSP, sealing surface sampling probe; ST, sulfatide; TAG, triacylglycerides, TCNQ, 7,7,8,8-tetracyanoquinodimethane THAP; 2,4,6-trihydroxyacetophenone; TLC, thin-layer chromatography; V-EASI; venturi-easy ambient sonic spray ionization

1. Introduction

Technological developments, particularly those in the field of mass spectrometry, have been central to the rapid growth in the field of lipidomics [1, 2] The ultimate goal of lipidomics is to quantitatively describe all lipids within a cell and their associated functions [3]. However, the extensive structural diversity observed in lipid populations poses a significant challenge to this endeavor. For example, variations in common structural motifs observed in mammalian lipids (*i.e.*, headgroup structure, chain length and degree of unsaturation in fatty acyl chains and the degree of sphingolipid glycosylation) have led to estimates of over 180,000 possible lipid structures in nature [4]. Moreover, isomeric variants arising due to alterations in double bond position, backbone substitution of fatty acyls, and stereochemistry, further increase the number of possible lipid structures. Thus comprehensive analysis of biological lipids requires analytical techniques possessing: (i) a high level of molecular specificity that allows one to differentiate the many molecular lipid structures invariably present in any lipid extract; and (ii) the ability to provide detailed structural information on the individual lipids present in a given system.

The excellent sensitivity and molecular specificity offered by modern mass spectrometry has made it arguably the method of choice for lipid analysis. No other analytical method allows for both the simultaneous and differential detection of individual lipid variants and acquisition of the detailed structural information that is required by the lipid researcher. Mass spectrometric analysis of lipids is traditionally achieved following lipid extraction from a sample (typically tissue or cells) and analysis by infusion-based electrospray ionization (ESI), with or without prior chromatographic separation. During ESI the sample solution is infused through a small capillary that has a high voltage applied (3-5 kV) [5]. This results in a charged spray being emitted from the capillary, which, following solvent evaporation assisted by a nebulizing gas, produces intact gas-phase lipid ions that then enter the mass

spectrometer for analysis. Once transferred into the mass spectrometer, lipid ions can be subjected to tandem mass spectrometry (MS/MS), primarily through collision-induced dissociation (CID). CID analysis readily allows the identification of a range of structural motifs, such as headgroup structure and the length and degree of unsaturation of fatty acid chains [6, 7]. These approaches have been invaluable for the structural, qualitative and quantitative analysis of lipids and form the foundation of most lipidomic workflows. For an in-depth discussion on the field of lipidomics and the role of mass spectrometry in lipid research please see references [1, 8].

In recent years there has been a plethora of new mass spectrometry approaches developed that provide direct surface analysis capabilities. These approaches allow direct detection of lipids from surfaces that are typically encountered in lipid analysis, such as tissue sections and intact cells, without prior extraction. Furthermore, many of these approaches can also be coupled with additional analytical techniques such as thin-layer chromatography (TLC), a popular method used for the separation of complex lipid extracts on a silica gel surface [9]. Perhaps the most powerful capability of these methods in regards to lipid analysis however, is their ability to acquire position-correlated spectra that allow the spatial distribution of lipids within a sample to be visualized (so-called mass spectrometry imaging or MSI). Thus surface analysis can provide complementary information to that typically obtained by infusion-ESI of biologically derived lipid extracts. Most notably, surface analysis can elucidate the spatial distribution(s) of lipids within a sample, complementing quantitative analysis on lipid extracts from the same source.

Regardless of the approach, there are three requirements for successful and efficient mass spectrometric surface analysis, namely: (i) desorption of desired analytes from the surface by the interaction of a sampling probe with the surface (*e.g.*, spray, laser, or plasma); (ii) ionization of desorbed analytes (note that some lipids, such as certain classes of

phospholipids, are already charged and do not require post-desorption ionization); and (iii) analysis of the gas-phase analyte ions in the mass spectrometer. Crucially, the energy deposited during the desorption and ionization events determines the structure of the detected ions (*i.e.*, fragments or intact molecules). Fortunately, for most (but not all) surface analysis methods, ionization is generally "soft". This means intact ions (*e.g.*, $[M+H]^+$, $[M+alkali]^+$, $[M-H]^-$) are the dominant ionic products. This is advantageous as the lack of fragmentation occurring during "soft" ionization produces easy-to-interpret spectra. For further structural information (*e.g.*, headgroup and fatty acid composition) these ions can then be subjected to collision-induced dissociation (CID) [6].

Traditional mass spectrometry surface analysis methods include matrix-assisted laser desorption ionization (MALDI) [10, 11] and secondary ion mass spectrometry (SIMS) [12]. Both methods have been used extensively for lipid analysis with great success, albeit with different capabilities. Importantly, in their conventional forms, MALDI and SIMS require desorption and ionization be performed *in vacuo*. This can complicate sample introduction and requires that the sample be resistant to modification in the vacuum environment (*e.g.*, dehydration of untreated tissue samples can lead to deformation, which may introduce artifacts). As a result, careful sample preparation is essential and often time consuming. Recently, the emergence of desorption electrospray ionization (DESI) [13] and direct analysis in real time (DART) [14] has catalyzed development of a vast array of mass spectrometry methods that allow direct surface analysis under ambient conditions (*i.e.*, at atmospheric pressure) [15-17]. Ambient techniques eliminate constraints associated with analyzing samples under vacuum and are characterized by simpler and faster analyses with minimal sample preparation requirements. Many of these methods have been applied to lipid analysis with varying degrees of success.

Lipid imaging of biological surfaces has been a very popular application of surface analysis mass spectrometry, particularly in bio-medical studies. However, given that lipid imaging by MALDI, SIMS and DESI has been the subject of several recent reviews [18-21], it will only discussed briefly here. Whether imaging is the focus or one simply wishes to characterize the lipids present on a given surface, a successful analysis is inherently dependant on the ability of the chosen method to desorb and ionize lipid molecules from the surface of interest. In this review we describe the mass spectrometry-based surface analysis methods for which lipid analysis has been demonstrated to-date and highlight the suitability of these techniques for the detection of the major lipid classes from different surfaces one may encounter during lipid research.

2. Laser-Based Methods

2.1 Matrix-Assisted Laser Desorption Ionization (MALDI)

Matrix-assisted laser desorption ionization was first reported in 1985 [22, 23] and is currently the most widely used technique for the detection of lipids directly from surfaces. This is evidenced by the fact that more than 250 papers have been published on the subject of lipid analysis by MALDI since 1997. These include applications as diverse as the investigation of lipid biochemistry by direct tissue analysis [19], to ageing processes in paintings [24]. MALDI samples can be prepared on a variety of substrates, including conventional stainless steel MALDI targets, TLC plates, or directly from biological surfaces such as tissue sections. Typically, lipid analysis by MALDI is achieved with one of two approaches: (i) Lipid profiling of extracts and tissue sections. This allows rapid comparisons of lipid composition to be made between different samples or within different regions of a tissue section; or (ii) MSI of tissues and other surfaces. MALDI-MSI is achieved by rastering the laser across the sample and acquiring mass spectra at each raster point, thereby generating an array of mass spectra across the sample. This allows the spatial distribution of many different lipids within the sample to be visualised in a single, label-free experiment. MALDI-MSI has been successfully applied to a wide range of tissues in a host of biological contexts. These include the analysis of changes in lipid composition and spatial distribution that occurs within diseased tissues. For more information on the biological applications of MALDI-MSI, the reader is referred to reference [19].

Desorption/ionization during MALDI typically occurs inside the vacuum region of the instrument and is initiated by a UV-laser pulse most commonly generated by a nitrogen (337 nm) or Nd:YAG (355 nm) laser (**Fig. 1a**). The typical spatial resolution of MALDI is ~25-100 µm which is largely defined by the diameter of the laser beam spot size on the target. The

laser serves two purposes: (i) to desorb analytes from the surface material; and (ii) induce analyte ionization for mass spectrometry analysis. While direct laser desorption is possible, the direct absorption of the laser energy by the analyte can lead to significant fragmentation and consequently low ion yields. Successful analysis thus requires the sample be coated in a matrix compound prior to laser irradiation, hence the term MALDI. Matrices are most often small, aromatic compounds with strong absorption characteristics at the laser wavelength. The matrix is commonly dissolved in a small amount of organic solvent and then applied to the sample, usually in the form of a spray or droplet, leading to the formation of matrix-analyte co-crystals [25]. The matrix serves two main purposes. Firstly, it facilitates extraction of analyte molecules from the sample leading to formation of analyte-matrix co-crystals. This step also separates and encapsulates individual analyte molecules, thus minimizing cluster formation during ionization. Secondly, the matrix serves to absorb the energy from the laser pulse, thus shielding analyte molecules and allowing soft ionization to occur. Upon UV-irradiation the matrix-analyte crystals are vaporized, and charge transfer reactions in the resulting plume lead to the formation of singly charged analyte ions typically in the form of $[M+H]^+$, $[M+alkali]^+$ or $[M-H]^-$.

The polarity of the generated ions is dependent on both the molecular structure (gas-phase acidity/basicity) of the analyte and matrix. Accordingly, positive ion formation typically requires an acidic matrix, while negative ion formation often requires a neutral or basic matrix. The presence of endogenous salts in biological tissue can also contribute to the formation of positive ions such as $[M+Na]^+$ and $[M+K]^+$, even in the absence of an acidic matrix. Optimal sensitivity is obtained with the formation of small analyte-matrix co-crystals, thus matrix application is one of the most critical steps in MALDI workflows. For example, sublimation of matrix produces a homogenous coating of small micro-crystals and was shown to provide *ca*. 50-fold improvement in signal for the analysis of phosphatidylcholine (PC),

specifically PC (16:0/18:1) compared to matrix application by electrospray, which produced much larger crystal sizes [26]. Furthermore, sublimation has proven to be a versatile and effective method for lipid analysis from a wide range of thin tissue sections [27]. Although not the focus of this review, it is important to emphasize that matrix application has particular significance in MSI as the crystal size, in addition to the laser spot size, limits the achievable spatial resolution. As lipids are extracted from the surface into the matrix layer, the size of the smallest biological features that may be resolved during an imaging experiment can be no smaller than the size of the crystals. Moreover, as most applications employ solvents, analyte migration may occur during matrix application and must therefore be minimized to preserve the spatial distributions within the sample. Therefore, methods that do not employ solvents, such as sublimation, are advantageous as the possibility of analyte migration is greatly reduced.

Table 1 outlines the lipid classes that have been detected by MALDI and the corresponding matrices. Clearly many types of matrices can be used for lipid detection, although presently 2,5-dihydroxybenzoic acid (DHB) and 9-aminoacridine (9-AA) are most commonly used for positive and negative ion analyses respectively [18, 28, 29]. The application of matrices to the sample also results in production of low mass (<500 Da) background ions that complicate the detection of low mass analytes. For this reason the detection of free fatty acids (FFAs) is particularly challenging using standard MALDI matrices. A variety of new matrices have been tested to overcome this and these are shown in **Table 1**. For example, due to its highly basic nature 1,8-bis(dimethylamino) naphthalene (DMAN) produces abundant $[M-H]^-$ ions of free fatty acids with little-to-no matrix background [65, 66]. **Fig. 2** shows negative ion spectra acquired from stearic acid (18:0) mixed 1:1 with (a) α-cyano-4-hydroxycinnamic acid (CHCA), (b) 2,5-dihydroxybenzoic acid (DHB) and (c) DMAN. The detection of the $[M-H]^-$ ion at *m*/z 283 (highlighted in red) is

difficult with both CHCA and DHB due to extensive formation of overlapping matrix-related ions. By contrast, *m*/z 283 is clearly observed using DMAN in the absence of any matrix interference .

As shown in **Table 1** and in several recent reviews [18, 19, 72-74], MALDI is capable of detecting virtually all major lipid classes. As with ESI, lipids such as PC, sphingomyelin (SM) and triacylglycerides (TAGs) are most efficiently detected in positive ion mode, whereas acidic lipids such as phosphatidylglycerol (PG), phosphatidylinositol (PI), sulfatides (ST) and gangliosides (GL) are better detected as deprotonated ions in negative ion mode. While some acidic lipids like phosphatidylserine (PS) and phosphatidylethanolamine (PE) can be analyzed in both polarities, positive ion analysis can suffer from the more rapid decomposition of $[M+H]^+$ ions and thus negative ion mode is usually preferred [75].

Most applications of MALDI (and many other methods) involve analysis of complex biological materials such as tissue or extracts containing many lipid classes. This can however introduce several complications:

First, in positive ion mode, the presence of endogenous salts within biological samples often results in the detection of several adduct ions for a given lipid. That is, a single molecular species may be observed simultaneously as $[M+H]^+$, $[M+Na]^+$ and $[M+K]^+$. This increases the likelihood of overlapping peaks (although in some cases this can be ameliorated with high resolution mass analyzers) and decreases sensitivity by spreading the signal of one analyte over several peaks with different *m/z* values. To overcome this, the matrix can be doped with salts, such as cesium [49] or lithium [76], to coalesce signals from an individual lipid variant into a single *m/z*. Alternatively, the sample can be washed with aqueous ammonium acetate (or similar) to remove salts leading to the sole detection of the protonated ion for lipids such as PC and SM [77]. The latter step is not suitable for all lipid classes as

removal of alkali salts may reduce the ionization of non-polar lipids such as TAGs that do not readily form protonated ions (although this may be offset by formation of ammonium adducts). Furthermore, as the aim of many tissue studies is imaging, care must be taken to avoid migration of the lipids from their original position in the tissue.

Second, the detection of some lipid classes in positive ion mode can be significantly hampered by the presence of overwhelming concentrations of PC and SM that can suppress the signal from less abundant and/or ionizable species, thus reducing the information obtained in a single acquisition [78]. In the case of extracts, several techniques can be employed to reduce ion suppression including: chromatographic removal of PC lipids by TLC [79]; cation exchange columns [80]; or by ensuring sufficient sample dilution [18]. An approach applicable for all samples is to perform analysis in negative ion mode where acidic lipid classes are detected with greater efficiency. For example, when Estrada *et al*. analyzed a human lens lipid extract in positive ion mode using PNA doped with cesium chloride as the matrix only several SMs were detected [39]. By contrast, negative ion analysis with a PNA matrix allowed detection of a much wider range of lipids including PE, lysophosphatidylethanolamines (LPE), PS, lysophosphatidylserines (LPS), ceramide-1-phosphates (Cer1P) and ST, highlighting the complementary information that can be obtained using both polarities. However, if one wishes to obtain the greatest amount of information from a lipid extract in a single acquisition, the coupling of MALDI with TLC provides a simple and effective method to achieve this. By separating lipid classes prior to analysis the suppression effects of PC/SM are eliminated and low abundance lipid classes (such as PI) can be observed even from complex samples [81]. TLC/MALDI has shown much promise for the analysis of both phospholipids (PLs) and glycosphingolipids (GSLs) from extracts obtained from a diverse range of sources [79, 81-85]. Nevertheless it may be affected by: (i) incomplete desorption of lipids from the plate due to the high affinity of some lipids for

silica; (ii) poor penetration of the UV-laser beam into the silica layer such that only lipids close to the surface are removed; and (iii) the possibility of ablating and contaminating the instrument with silica. In addition, TLC analysis generally requires more material than a simple profiling experiment where the sample is spotted directly onto a standard MALDI plate. One must also be aware of the possibility of oxidation of surface-exposed unsaturated lipids upon exposure to atmospheric ozone [86].

In an effort to overcome problems associated with lipid detection from the silica surface, Goto-Inoue *et al*. developed a TLC-blot technique whereby lipids separated by TLC are transferred to a polyvinylidene difluoride (PVDF) membrane. This facilitated more efficient desorption in the MALDI analysis and has successfully been employed for the characterization of biologically derived GSL [87] and PL [34] extracts with detection limits as low as 1 pmol. **Fig. 3a** shows a primuline stained TLC plate following separation of lipid extracts derived from four different regions of the human brain [34]. Upon primuline staining ~12 different lipid classes were visualized on the TLC plate and then transferred to a PVDF membrane and interrogated by MALDI-MS to acquire molecular information. **Fig. 3a and Fig. 3b** show MALDI spectra acquired from the highlighted bands containing PC and SM lipids and readily allow identification of multiple molecular lipids present in a given band. MALDI analysis also allowed the identification of bands containing, PE, PS, galactosylceramides (GalCer) and ST in positive ion mode using DHB as the matrix. MALDI spectra from the remaining TLC bands were not reported, however it is likely these bands correspond to a variety of other GSLs (*e.g*., lactosylceramides (LacCer) and GLs) and acidic phospholipids such as PI. Additionally, by comparing the abundance of ionized SM in different brain regions, the relative distribution of SM lipids in these regions could be inferred. For example, it was observed that SM (d18:1/20:0) was more abundant in grey

matter, SM (d18:1/24:1) was more abundant in the white matter while SM (d18:1/18:0) was distributed evenly throughout the tissue.

Another approach to acquire more information in a single MALDI experiment is by combining ion mobility separation with mass analysis. Ion mobility induces molecular-level separations based, in part, on the collision cross section (determined by shape and size) of the ions. The separation occurs between the ionization and mass analysis events and typically occurs on the millisecond timescale. Different molecular classes generally exhibit different collisional cross sections and this can be exploited to separate lipids-related ions from other ionized species such as matrix-related ions, metabolites and peptides [88]. Furthermore, ion mobility has been shown to be capable of separating different phospholipid classes and even to allow intra-class separations based on fatty acid chain length, degree of unsaturation and nature of binding to the glycerol backbone (*i.e.*, esters, alkyl ethers and vinyl ethers) [88-90]. This allows one to identify and distinguish certain isobaric lipids. For example, Jackson *et al*. demonstrated the ability to distinguish the gangliosides structural isomers, GD1a and GD1b [91]. The differentiation of more subtle variations within complex lipids, such as double bond position, has yet to be demonstrated using ion mobility alone. It should also be noted that while ion mobility can reduce chemical noise, it occurs after ionization and thus does not alleviate ion suppression effects.

Advances in the sensitivity of MALDI-MS technology now allow lipid analysis to be performed at the single cell level. As an example, MALDI has recently been used to investigate the lipid compositions of single oocytes [58] and individual fly egg chambers [42]. Ferreira *et al*. successfully acquired PC, SM and TAG lipid profiles directly from intact oocytes and with sufficient signal to acquire tandem mass spectra (MS/MS) for structural identification [58]. Human and other animal derived oocytes were analyzed and lipid profiles found to be characteristic of species. For example, human, bovine and sheep oocytes were

dominated by PC (34:1), although bovine oocytes showed a higher signal for several TAGs. By contrast, fish oocytes contained significantly elevated levels of polyunsaturated lipids such as PC (38:6) and PC (40:6)

At present, MALDI-MS is the most widely used method for the surface analysis of lipids, but there is still room for further development. The complementary information acquired using both positive and negative ions often requires parallel analysis of the same sample and thus a different matrix and sample preparation step for most efficient ionization in each polarity. It is therefore desirable to use a matrix allowing efficient ionization in both ionization modes. Although some common acidic matrices are also capable of generating negative ions (see **Table 1**), promising results using 1,5-diaminonapthalene [31] and acid/base doped binary matrices [92] for the efficient ionization of lipids in both polarities have recently been reported. Additionally, the need to place the sample inside the vacuum region of the instrument not only complicates sample introduction but can also result in the loss of volatile analytes/matrix and change sample morphology due to dehydration. The recent application of atmospheric pressure MALDI to the analysis of lipids can overcome this limitation.

2.2 Atmospheric Pressure MALDI (AP-MALDI)

Atmospheric pressure MALDI (AP-MALDI) was first reported in 2000 [93] and shares many similarities with conventional vacuum UV-MALDI including the use of the same matrices. The difference stems from desorption/ionization occurring in the ambient environment prior to ion transfer into the vacuum region of the mass analyzer. In terms of lipid analysis, one of the main advantages of AP-MALDI over vacuum MALDI is the collisional cooling of ions (*i.e.*, the facile removal of ion internal energy by collisions with a

neutral gas) during transfer at atmospheric pressure. This results in less fragmentation than conventional MALDI [93, 94]. However, this phenomenon can also lead to undesirable matrix/analyte cluster formation [93]. Other advantages of AP-MALDI include: (i) the ability to easily interchange an AP-MALDI source with other ionization sources; (ii) the capability to analyze compounds and alternative matrices that are not stable under vacuum conditions; and (iii) the ease of introduction and subsequent access to the sample plate resulting in higher throughput and the ability to manipulate the sample during analysis. Nevertheless, AP-MALDI is generally less sensitive than vacuum-MALDI due to ion losses during transfer from the ambient environment into the instrument, although ion transmission efficiency can be improved through pulsed dynamic focusing [95]. Trimpin *et al*. have also described a field-free transmission geometry to improve ion transmission efficiency [96]. In this geometry matrix is present between a glass slide and tissue section and the laser fired at the back of the glass slide with the resulting plume carried into the mass spectrometer by diffusion.

AP-MALDI has successfully been applied to the analysis of retinal lipids [97], GLs [98], plant tissue [99], and animal tissue [96, 100]. Furthermore, recent applications of AP-MALDI using tightly focused laser beams (spot size ~5-7 µm) has allowed the lipid composition of single cells, including HeLa cells [101] and individual cells within salamander retinal tissue [97], to be studied. Using this approach, Roy *et al*. observed distinct lipids compositions within the different cellular layers of salamander retinal tissue [97]. For example, monounsaturated and saturated lipids such as PC (32:1) and PC (32:0) were distributed primarily in the outer and inner plexiform layers while polyunsaturated PC lipids such as PC (36:4), PC (38:6) and PC (40:6) were observed mainly in the retinal pigment epithelium, outer segment and inner segment cellular layers. Analysis of GLs by AP-MALDI is particularly advantageous as in-source fragmentation during vacuum-MALDI results in the

loss of the sialic acid group [102, 103]. Collisional cooling of GLs generated by either intermediate pressure MALDI with source pressures in the millibar range [103], or AP-MALDI [98], can significantly reduce the extent of in-source fragmentation.

2.3 Infrared MALDI (IR-MALDI)

The fundamental principles of infrared MALDI (IR-MALDI) are identical to those of conventional UV-MALDI, with the exception than an IR laser is used: commonly Er:YAG or OPO lasers emitting at 2.94 μm. Additionally, the spatial resolution of IR-MALDI is typically ~100-300 μm which is lower than UV-MALDI. The longer wavelength means matrices used for IR-MALDI can be different to those used for UV-MALDI. At 2.94 μm the laser is coincident with the OH-stretch vibrations of bulk water and glycerol and, as such, these are commonly used as IR-MALDI matrices [104, 105]. The ability to use liquid matrices negates the requirement for analyte-matrix co-crystallization, a critical step with solid UV-absorbing matrices. Moreover, as application of organic solvents and acids is not required for the analysis, chemical alterations of the sample surface are minimized. IR-MALDI has been coupled to both vacuum and atmospheric pressure ion sources. Along with the obvious advantages of an atmospheric pressure source (see AP-MALDI), AP-IR-MALDI permits the use of endogenous water as a matrix [106], allowing direct analysis of samples in their natural state and with their endogenous chemical composition. Shrestha *et al*. applied this approach to the analysis of mouse brain tissue and readily detected 79 lipids and metabolites, including a variety of PLs, diacylglycerides (DAGs) and cholesterol [107]. In an earlier study, Dreisewerd *et al*. used intermediate pressure IR-MALDI for direct analysis of rat brain tissue without an external matrix and detected a variety of PL and GSL classes [108]. Detection of PLs and TAGs from plant material has also been demonstrated [109,

110]. As is commonly observed in UV-MALDI, fragmentation of the PC headgroup is also a feature of IR-MALDI.

IR-MALDI is particularly advantageous for the analysis of lipids separated on TLC plates due to the high penetration depth of the laser (typically several microns) [111]. This is much greater than laser penetration depths achieved using UV-MALDI (~50-200 nm) [112], and leads to the sampling of much more material per pulse in the former technique. However, it is important to note that the same effect can lead to rapid sample depletion and also increases the likelihood of silica contamination of the ion source. TLC/IR-MALDI has been successfully demonstrated for the direct analysis of TLC-separated lipid mixtures consisting of PLs [113] and GSLs [114, 115]. Rohlfing *et al*. readily detected cardiolipin, PG, PE, phosphatidic acid (PA), PC and SM after spotting glycerol onto the bands of interest [113]. Detection limits of 5 and 50 ng were determined for SM and PG in positive ion mode, respectively. A disadvantage of this approach was the detection of individual lipids as multiple ion signals including $[M+H]^+$, $[M+Na]^+$, $[M+K]^+$ and even glycerol adducts. Such adduct formation results in unnecessarily complex spectra with lower signal-to-noise, even when only a few unique lipids were present at a given sampling spot. Glycerol adducts have also been observed for GL analysis in negative ion mode [114], and are attributed to the use of an elevated pressure ionization source and associated collisional cooling of the adducts. The use of an elevated pressure ion source (0.1-0.5 mbar), in combination with IR-MALDI, was also found to greatly reduce the extent of in-source fragmentation and lead to the primary observation of intact gangliosides with a reported GM3 detection limit of 50 ng for GM3. Material ablation by IR-MALDI has recently been utilized to transfer lipids from a tissue section onto a nitrocellulose substrate for subsequent UV-MALDI analysis [116]. This has the advantage of minimizing alkali adduct formation and can also allow pre-concentration of surface-bound lipids prior to secondary analysis.

Despite the aforementioned advantages, IR-MALDI has not experienced the same level of popularity as UV-MALDI. One possible reason may be that the greater amount of material ablated with IR-MALDI per laser pulse makes it difficult to implement on instruments designed for UV-MALDI operating at high vacuum with high field strengths [117, 118]. Nonetheless, the ability to use endogenous water as a matrix makes IR-MALDI particularly well suited for the analysis of lipids directly from tissues without an external matrix. In addition, the greater laser penetration depth means IR-MALDI is also well suited for analysis of TLC plates using a glycerol matrix, while there are also numerous reports of successful application of intermediate and atmospheric pressure sources [107, 109, 110, 113-115].

2.4 Laser Desorption with ESI Post-Ionization

In recent years a variety of laser desorption techniques coupled with post-ionization by ESI have been developed, namely matrix-assisted laser desorption electrospray ionization (MALDESI) [119], laser ablation electrospray ionization (LAESI) [120] and electrospray laser desorption ionization (ELDI) [121]. These methods are closely related and differ only by the use of an IR laser (LAESI), UV-laser (ELDI) or an external matrix (MALDESI). These approaches serve to make use of the dominant production of neutral species during laser desorption by capturing the plume and ionizing neutral species within an electrospray orientated perpendicular to the laser beam, leading to enhanced ion yields. The electrospray is generated by infusing a polar solvent through a small diameter capillary to which a high voltage is applied. The high electric field created at the capillary tip leads to the creation of a fine spray of charged droplets (the electrospray) [5]. As these charged droplets intersect the ablation plume, desorbed molecules become encapsulated and eventually form intact, gas-phase ions upon solvent evaporation. A schematic diagram of the LAESI process is shown in

Fig. 1b. Alternatively, the plume can be captured in a suspended droplet above the irradiated area and subsequently subjected to ESI analysis [122]. These techniques have been applied to the analysis of lipids (mostly PLs) from a variety of substrates including tissue [107, 123-125], cell pellets [126] and chicken egg yolk [119]. The LAESI approach has found application for single cell analysis [127, 128]. Single cells (plant and human cheek cells) were first targeted by optical microscopy and then ablated by a 2.94 μm laser pulse focused though a glass optical fiber tip. The focused laser produced ablation areas of 30-40 μm in diameter, allowing for the targeted analysis of the large individual cells with dimensions of *ca*. 300 x 50 μm. The plume was then ionized by ESI, leading to the detection of metabolites in addition to the tentative detection of several DAGs and monoacylglycerides (MAGs). The ability to detect molecules from single cells highlights the excellent sensitivity that can be achieved with this method. In addition, a recent study has demonstrated sensitivity improvements for the analysis of non-polar lipids such as sterols, TAGs and cardiolipin by employing an ESI source with a heated nebulizing gas (~170-220°C) [129]. Such developments help increase the range of lipid species suitable for analysis with both LAESI and other spray-based techniques. LAESI is a promising approach for the detection of intact lipids from both biological tissues and individual cells under ambient conditions without an external matrix. With the ability to accurately target an individual cell within a tissue, this approach (and indeed other laser-based methods) may be capable of investigating changes in the cellular lipidome with changing micro-environment (*i.e.*, position in tissue), although tighter laser focusing will be required for such analyses of smaller mammalian cells.

2.5 Matrix-Free Laser Desorption/Ionization Approaches

MALDI has proven to be an extremely successful method for surface analysis of lipids. However, the need to apply a matrix leads to the production of matrix-related ions which can complicate the interpretation of the spectrum. It also introduces an additional sample preparation step and thus represents a limitation of the technique. As such, there has been interest in the development of methods that permit soft laser desorption/ionization from surfaces without a matrix. These techniques use an active nanostructured surface to couple the laser energy to the desorption/ionization of analytes present on the surface [130]. These surfaces are typically composed of carbon or silicon and replace the standard MALDI target plates. Once the sample is mounted upon the surface it is usually analyzed by traditional vacuum MALDI instrumentation. A variety of similar approaches have been described including desorption/ionization from porous silicon (DIOS) [131], nanowire-assisted laser desorption ionization (NALDI) [132], nanostructure-initiator mass spectrometry (NIMS) [133] and graphite-assisted laser desorption ionization (GALDI) [134], with the primary difference between the techniques being the type of substrate. Additionally NIMS uses a porous, nanostructured silicon substrate doped with an "initiator" molecule, typically siloxanes or silanes [133, 135]. The primary advantage of these techniques compared to standard MALDI is the production of significantly fewer matrix-related ions in the resulting spectrum, greatly simplifying the detection of low mass compounds such as FFAs [136, 137]. Here we will focus on the two most recent methods, NALDI and NIMS (**Fig. 1c**). For optimal detection these require lower laser fluence than that deployed in traditional UV-MALDI, suggesting the nanostructured surface is more efficient at coupling the laser energy to the target substrate while minimizing in-source fragmentation of ionized analytes. Furthermore, where direct comparisons are available, these approaches can provide equivalent or even greater sensitivity than MALDI [131, 138-140].

NALDI uses silicon nanowire substrates and was first reported in 2005 [132, 141]. Depending on the nanowire structure, NALDI can produce ions with lower internal energies than can be achieved with either MALDI or DIOS approaches [132]. Along with minimizing analyte fragmentation, the lower laser energy also produces very few surface-related background ions. This enhancement may result from the focusing of laser energy at the tips of the nanowires, more efficient heating of the sample/surface, or a combination of the two. NALDI has been used for the analysis of a variety of lipids including PLs, TAGs, DAGs and FFAs derived from both standards and biological extracts [136, 142-144] in addition to PLs from tissue sections [145] and gecko footprints [146]. To highlight the sensitivity improvements that can be achieved with NALDI, Muck *et al*. demonstrated a 200-fold increase in signal for analysis of TAG (16:0/16:0/16:0) doped with lithium relative to analysis of an equimolar solution by conventional MALDI using LiDHB as the matrix [136].

Desorption/ionization in NIMS occurs following irradiation of adsorbed analytes usually by a UV-laser, although ion beams (see section 3 below) also been used [133]. This induces rapid heating of the surface causing initiator molecules to vaporize and induce desorption and ionization of surface-bound analytes. In a direct comparison of MALDI, ESI and NIMS for the detection of lysophosphatidylcholine (16:0), NIMS was capable of detecting as little as $5x10^{-17}$ moles whereas MALDI and ESI were found to have $>10^{-15}$ mole limits of detection [133]. NIMS has been successfully employed for the analysis of a range of compounds such as metabolites and various lipids including PLs, GSLs and sterols, from a range of complex samples including blood, urine, saliva, and even single cells with greater sensitivity than MALDI [133]. Direct tissue analysis of PLs and cholesterol has also been demonstrated [147, 148]. For example, Lee *et al*. have described the use of NIMS for the detection and imaging of lipids from mouse brain tissue [148]. Tissue slices (5 µm thick) were prepared, placed onto the NIMS surface and then directly analyzed with a commercial

MALDI system. A variety of PC lipids were readily detected and alterations in lipid composition across the tissue allowed a variety of brain regions to be readily resolved, including glial and neuronal cell enriched regions. Results were also supported by histological staining. It is important to note that direct tissue analysis by any of the matrix-free methods described above requires thin sections (<12 μm) to facilitate transmission of the laser pulse through the tissue to the active surfaces. However, this can require more stringent sample preparation requirements and some tissue types may not be well suited for preparing such thin slices. In some cases direct laser desorption of biological samples can be performed without an external substrate. Recently Yew *et al*. [149] described the direct UV-laser desorption from insect cuticles. It is believed that the microstructure of the insect body itself acts as the active surface facilitating analyte desorption/ionization [150]. Direct laser desorption from insect cuticles was used for detection of endogenous alkene-based pheromones and TAGs [149, 150].

The ability to softly ionize and detect lipid molecules from tissues and extracts with greater sensitivity and in the absence of interfering background ions using matrix-free soft laser desorption/ionization is an exciting development. Perhaps the major obstacle preventing wider uptake of these methods is the need to fabricate suitable surfaces. Increasingly however, these surfaces can be prepared using well described protocols and NALDI substrates are now commercially available. Additionally, the demonstration that naturally occurring substrates, such as insect cuticles, can act as NALDI targets may serve to further increase the accessibility of these approaches.

3. Secondary Ion Mass Spectrometry (SIMS)

In secondary ion mass spectrometry (SIMS), a sample surface under high vacuum is bombarded with an energetic primary ion beam (typically 1-40 keV). Samples are usually mounted onto steel, glass or silicon substrates. As the ion beam strikes the surface a collisional cascade involving atoms and molecules within ~10 nm of the surface is initiated, ultimately leading to ejection of material from the surface [151, 152]. The released material consists of neutrals, electrons and ionized species. These so-called secondary ions typically represent less than 0.1% of the total ejected material. The ion beam can be focused down to ~100 nm (in the case of atomic ion sources) [153], allowing the spatial distribution of surface molecules to be investigated with resolution far beyond that possible with laser and spray-based methods. Nevertheless, larger beam sizes (>200 nm) are often used for the analysis of tissue and cells in order to increase sensitivity. SIMS does not require the application of a matrix, although use of MALDI matrices and other surface treatments can lead to significant improvements in sensitivity (see later). Nonetheless, careful sample preparation of biological surfaces such as tissue and cells is critical. Care must be taken to ensure no deformation due to dehydration of the sample occurs when it is introduced into the vacuum region. Care must also be taken when mounting/preparing samples to ensure no height profile artifacts are introduced. Additional care must be taken when mounting cells for analysis in order to avoid analyte delocalization [154]. Methods for the preparation of biological samples for SIMS have been covered in a recent review by Passareli and Winograd and usually involve cryofixation, sectioning and freeze drying for tissue and frozen hydration for cells [21].

SIMS experiments can be performed in either static or dynamic mode, although static SIMS is used almost exclusively for lipid analysis [21]. Static SIMS uses primary ion fluxes less than 10^{13} ions.cm^{-2} usually generated with a pulsed-ion beam. Under static SIMS conditions less than 1% of the surface molecules are exposed to the ion beam. This minimizes

the chance of analyzing the same region twice, thus increasing the probability of detecting molecular ions, as each new region has not been damaged by a prior beam impact. Even under these conditions, the energetic desorption process often results in extensive molecular fragmentation. This means that intact lipids are seldom observed using atomic ion sources, although the development of cluster ion sources has helped to reduce this effect (see below). As a result SIMS is not suitable for the lipid profiling of biological tissue and extracts. For profiling experiments, "softer" desorption/ionization approaches such as MALDI and DESI (see section 4.1) are much better suited. Nonetheless, the unique ability of SIMS to acquire spatially resolved molecular information at sub-micron resolution (compared to laser-based methods with typical resolutions of 25-200 μm) has brought about interest in SIMS for lipid analysis, in particular imaging of tissue sections and single cells.

Early SIMS experiments used atomic ions sources such as Ar^+, In^+ and Ga^+, however analysis of biological compounds resulted in extensive molecular fragmentation and suffered from low secondary ion yields. Despite this, lipid classes could be detected even from single cells by virtue of class-specific fragment ions such as the phosphocholine fragment at *m/z* 184 that is characteristic of PC and SM [155-157]. In one study an indium primary ion beam focused to a 200 nm diameter was used to study lipid changes observed in the fusion region during tetrahymena mating [155]. Cells were prepared by cryogenic freezing and freeze-fracturing under high vacuum conditions, thus ensuring the cell structure was maintained for analysis. The relative abundance of several lipid-related fragment ions, namely: *m/z* 69 ($C_5H_9^+$), a hydrocarbon fragment characteristic of total phospholipid; *m/z* 184 characteristic of PC and SM; and *m/z* 126 characteristic of 2-aminophosphonolipid (2-AEP), was mapped as a function of position within the mating cells. While total phospholipid content did not show a significant alteration in the mating region relative to the cell bodies, a decrease in PC was observed in the junction region of the mating cells (average decrease of 67±7% between

the cell bodies and conjugation junction across 8 samples). This decrease in PC in the junction region correlated with a relative increase in 2-AEP, as observed both by principal component analysis (PCA) and a relative increase in the characteristic 2-AEP-related ion within the junction region. A common observation using tightly focused atomic ion sources for the analysis of biological surfaces is the low bio-molecular ion yields [158]. As a result, care must be taken when making conclusions based on ion abundances. In this study, the observation of similar trends in multiple samples, in addition to similar observations with PCA, increases confidence in the analysis.

The advent of cluster ion sources generating primary ions such as Au_3^+, Bi_3^+ and C_{60}^+ has significantly increased the utility of SIMS for intact lipid analysis [159-161]. Cluster ion sources generate a significant increase in the amount of material ejected from the surface upon projectile impact, thereby providing more material for the analysis. In addition, they also lead to higher ion yields, reduced surface damage and enhanced observation of intact lipid ions relative to ionic fragments [158, 159, 162, 163]. In the case of C_{60}^+, the reduced surface damage allows a stable, prolonged ion signal at a fixed sampling position and enhanced signal with acquisition using higher ion fluences, thereby allowing analysis of a larger portion of the sample area [163]. As the cluster breaks up upon surface impact the initial energy is spread across multiple smaller fragments, and unlike atomic sources, cluster ions are capable of depositing a significant portion of the cluster energy close to the surface [164]. These effects are responsible for the softer desorption/ionization processes observed with cluster ion sources. The higher secondary ion yield and lower extent of fragmentation produced by C_{60}^+ ion beams [158] results in them showing much promise for the analysis of intact lipids. The higher secondary ion yield and lower extent of fragmentation produced by C_{60}^+ ion beams [158] shows promise for the analysis of intact lipids.

To highlight the enhanced molecular sensitivity offered by C_{60}^+, Ostrowski *et al.* compared the intensity of lipid-related ions obtained from C_{60}^+ and Ga^+ ion sources and found 70-1000 fold signal enhancement for the C_{60}^+ ion source with the degree of enhancement dependant on lipid class [162]. In another study, rat brain tissue was analyzed using both Au^+ and C_{60}^+ ion sources [163]. The C_{60}^+ ion source allows the detection of cholesterol (*m/z* 369 and 385) and a range of intact phospholipids from *m/z* 700-800 with a significantly higher signal than that obtained from the Au^+ source (**Fig. 4**). In a similar analysis involving rat cerebellum using a Bi_3^+ cluster source, intact ions corresponding to cholesterol, PC and GalCer lipids were observed [165]. Lipid classes detected as intact ions from mammalian tissues include PLs, glycerolipids, fatty acids, sterols, prenol lipids and sphingolipids [21]. However, not all species in each class have been detected. For example, intact PE and cholesterol esters have not been detected by SIMS, most likely due to the facile loss of the PE head group and cholesterol ester chain, respectively. Although intact PE lipids have been detected by MALDI, loss of the headgroup has also been reported [75]. Detection of intact lipid ions using SIMS from single cells is more challenging, largely due to the limited amount of material available for analysis. Unlike softer ionization methods applied to single cell analysis, often only class-specific fragment ions are observed making it to difficult to acquire information on individual molecular species [21].

In efforts to improve the ion yields obtained by SIMS and to enhance its capability for bimolecular analysis, several surface treatment methods, namely matrix-enhanced SIMS (ME-SIMS) and metal-assisted SIMS (Met-SIMS), have been developed. ME-SIMS requires the sample be coated in a MALDI matrix such as DHB [166-168], which leads to both enhanced ion yields and softer ionization. ME-SIMS spectra resemble those acquired by MALDI, suggesting that gas-phase charge transfer is a contributor to the enhanced ion yields [169]. An important advantage of ME-SIMS is the ability to detect intact lipids using atomic

ion sources such as indium instead of the more expensive cluster ion sources [167, 169]. Complications associated with ME-SIMS arise from the matrix application which can lead to analyte delocalization, hot-spots associated with matrix crystallization and a reduction in spatial resolution dependent on the matrix crystal size [170]. Furthermore, the matrix produces ions that can interfere with lipid detection. Ionic liquid matrices have been shown to eliminate hot-spots as no crystallization occurs, and can provide up to a 1000-fold increase in sensitivity relative to native samples for the detection of intact PC, PE and cholesterol [171].

Met-SIMS involves the coating of the sample with a thin layer of metal (~1 nm) such as gold or silver [172, 173]. As no solvents are used, Met-SIMS provides enhanced biomolecular ion yields without delocalization. Analysis of rat kidney tissue coated with a thin layer of silver and ionized with a Ga^+ ion beam revealed enhanced cholesterol detection with sub-cellular resolution [173], while positive ion analysis of rat brain tissue using Bi^+ and Bi_3^{2+} beams resulted in enhanced detection of positive ion cholesterol and intact PLs when the tissue was coated with gold [172]. Interestingly, negative ion analysis using Bi^{3+} produced higher signal intensity from untreated tissue sections, highlighting a disadvantage of Met-SIMS - namely the difficulty in predicting which ions will be enhanced. Analysis of single neuroblastoma cells using gold Met-SIMS with an $^{115}In^+$ beam reveals many ions up to *m/z* 1200 that are detected from the cell surface [174]. Of these, only cholesterol and a DAG could be identified due to extensive adduct formation with the coating material. Nonetheless, the ability to detect intact biomolecules from tissue and cells is an important development towards the improved capability of SIMS for direct lipid analysis.

The capabilities of SIMS for lipid analysis have recently been further enhanced with the development of new time-of-flight instrumentation allowing MS/MS acquisition, high mass resolving power and greater compatibility with continuous cluster ion sources by decoupling the mass spectrometric analysis from the desorption event [175-177]. Traditional time-of-

flight SIMS instruments required short (nanosecond) ion beam pulses to ensure high mass resolution. This came at the cost of duty cycle and analysis time and thus made them incompatible with continuous cluster ion sources. Furthermore, the inability to acquire MS/MS spectra severely limited the ability of such systems to identify ions. These recent advances allowing both high mass resolving power and MS/MS acquisitions have greatly improved the ability to identify unknown lipids and resolve signals from molecular species with the same nominal mass. Despite these advances and unrivalled spatial resolution, SIMS does not enjoy the popularity of MALDI or ambient ionization approaches such as DESI (see section 4.1) as a routine method for lipid analysis. The often extensive fragmentation observed is a likely contributor to this as it limits the ability to acquire comprehensive molecular lipid profiles. Moreover, the low ion yields, particularly at high spatial resolution, may limit the ability to identify many lipids through MS/MS. While ME-SIMS and Met-SIMS may partially resolve this issue they introduce additional sample preparation steps. Nonetheless, SIMS is currently the only MS-based method providing sub-micron spatial resolution and allowing the distribution of lipids across a cell surface, including 3-D lipid distributions, to be investigated [154], and thus represents an important tool for lipid analysis.

4. Liquid Extraction and Spray-Based Methods

In this section we describe methods that rely on the liquid extraction and subsequent ionization of surface-bound analytes. Ionization either occurs concomitant with the extraction (spray-based methods) or subsequent to the extraction step (liquid extraction methods). Importantly, in all approaches analysis is performed under ambient conditions, thus reducing analysis times and simplifying sample introduction. An important attribute of these approaches is the continuous generation and introduction of ions into the mass spectrometer, in contrast to the pulsed-ion generation achieved with most laser-based and ion-beam

approaches. This makes liquid extraction and spray-based methods well suited for coupling with many different mass analyzers and more amenable to MS/MS experiments. This is advantageous for both detailed structural analysis as well as comprehensive lipid profiling incorporating the precursor and neutral loss scans commonly deployed in conventional shotgun lipidomics [8]. These targeted MS/MS scans allow the sensitive detection of lipids with a particular structural motif (*e.g.*, headgroup or fatty acyl composition), and are achieved by the detection of either a characteristic charged fragment (precursor ion scan) or the corresponding loss of a neutral fragment (neutral loss scan). ESI is by far the most common ionization method, however others such as atmospheric pressure chemical ionization (APCI) have been demonstrated. These approaches are also compatible with most commercial instruments with the only modifications required being those for the initial liquid extraction step.

4.1 Desorption Electrospray Ionization (DESI)

Desorption electrospray ionization (DESI) was the first of the spray-based surface analysis methods to be described and is arguably the most widely used ambient ionization technique [13]. DESI analysis is performed under ambient conditions using a pneumatically assisted electrospray directed at the surface of interest. Charged droplets impinge the surface where they facilitate analyte dissolution and generate secondary droplets containing dissolved surface-bound analytes (**Fig. 5a**). These droplets are scattered off the surface under the influence of the nebulizing gas, with the analytes subsequently ionized by ESI-type mechanisms involving solvent evaporation and charge retention. The main strengths of DESI stem from its ability to directly analyze surfaces under ambient conditions with minimal sample preparation, while also allowing the soft ionization of biomolecules such as lipids and

proteins. The achievable spatial resolution is determined largely by the diameter of the spray at the surface and is typically 200-500 μm, although spatial resolutions as low as ~40 μm have been reported under certain conditions [178, 179].

Fluid dynamics simulations have been employed to elucidate the precise desorption mechanisms of DESI [180, 181]. A droplet-pickup mechanism is accepted as the dominant mechanism responsible for DESI. Costa *et al*. [180] revealed that as charged droplets are directed at the surface an initial thin solvent layer is formed. This solvent layer extracts and dissolves surface analytes. The continuous flow of droplets at the surface leads to the release of secondary droplets containing liquid from both the incoming droplets and the liquid film containing the analyte(s) and it is from these droplets that gas-phase analyte ions are created and analyzed.

Owing to its ability to readily desorb and ionize lipids from a variety of surfaces including glass, poly(methyl methacrylate) and polytetrafluoroethylene (PTFE) [182], tissue sections [20] and silica TLC plates [183, 184], lipid analysis has become one of the most popular applications of DESI. Early studies focused on optimization of solvent composition and surface structure to enhance the sensitivity of lipid detection from standards and extracts [182]. It was found that 1:1 methanol:water mixtures and PTFE surfaces provide the highest and most stable signal for deposited lipids in both positive and negative ion modes. This was attributed to the larger spray diameter using methanol/water mixtures resulting in a larger desorption area.

Table 2 lists the major lipid classes and corresponding surfaces analyzed by DESI-MS. Most major lipid classes have been successfully detected by DESI, with one notable exception being wax esters. With the exclusion of cholesterol that is commonly detected as the $[M+H-H_2O]^+$ ion, all other classes can be detected as intact ions with little fragmentation.

While many studies have used DESI for the analysis of lipid mixtures (extracts and tissues sections), it is crucial to note that DESI is still subject to the same ion suppression effects arising from abundant fixed charge PC and SM lipids that were previously described for MALDI. Recent analysis of human lens tissue by both MALDI [54] and DESI [185] however, may indicate that under typical conditions DESI is less susceptible to these effects than MALDI and thus allows detection of a wider variety of lipid classes in a single acquisition. For example, positive ion mode MALDI (using DHB as the matrix) detected only SM, ceramide (Cer) and cholesterol lipids whereas DESI (using 4:1 MeOH:H_2O + 0.05% hydrochloric acid as the spray solution) detected SM, Cer, Cer1P, PE, LPE, PS, LacCer and cholesterol.

The ability to use the same spray solution for acquisition of both positive and negative ion data is advantageous when compared to MALDI, which often requires different matrices for most efficient ionization with each polarity. The spray can also be doped with a small amount of acid or salt to aid ionization. Examples of this include sodium or ammonium salts for detection of TAGs [195], ammonium formate for analysis PC and SM in negative ion mode [182] and silver ions for olefins [197]. In the latter study, the addition of silver nitrate to the DESI spray solvent resulted in an order of magnitude increase in sensitivity for the detection of unsaturated FFAs, fatty acid esters and prostaglandins from a PTFE substrate as $[M+Ag]^+$ ions when compared to the abundance of ionized lipids generated with an undoped spray. Additionally, this approach allowed the detection of FFAs and TAGs in positive ion mode from dog bladder tissue. In contrast, a previous study using 1:1 acetonitrile:water spray solution for the analysis of the same tissue type did not reveal the presence of TAGs [192].

The composition of the spray can also be manipulated by adding a reagent that selectively reacts with a target analyte and enhances its detection. This is referred to as "reactive DESI" [203-207] and it has been used for the detection of cholesterol and other

hydroxyl-functionalized non-polar lipids such as steroids and some vitamins. Due to its low polarity and lack of ionizable functional groups, intact cholesterol is not readily observed by electrospray-based methods. Wu *et al*. [199] doped betaine aldehyde into the spray solution which upon desorption from the surface (PTFE, glass and tissues section) reacted with cholesterol within the micro-droplets. The reaction produces a hemiacetal with a fixed-positively charged trimethylammonium group and provides a 0.5 ng detection limit for cholesterol. **Fig. 6a** shows a reactive DESI experiment on a rat brain allowing simultaneous detection of intact cholesterol and phospholipids. This approach has also found success for the rapid quantitation of cholesterol in human serum deposited onto glass [199]. In this analysis quantitation was performed using standard addition with known amounts of cholesterol and D_7-cholesterol doped into the serum samples. This resulted in a relative standard deviation of 1.2-6.4 % and calculated cholesterol quantities comparable with more established gas-chromatography and ESI-MS approaches. When coupled with discharge-induced oxidation, reactive-DESI has also proven effective for the analysis of saturated hydrocarbons where *in situ* oxidized hydrocarbons react with doped betaine aldehyde [208]. The detection of hydrocarbons from a vacuum oil distillate using this technique is shown **Fig. 6b**.

The ability to simply deposit biological material and analyze it in the open environment by DESI allows the rapid lipid profiling of biological samples. This approach has been utilized for the rapid analysis of micro-organisms such as bacteria [189, 209]. Zhang *et al*. investigated four different strains of bacteria by simply depositing several microlitres of a bacterial suspension onto a glass slide with subsequent analysis by DESI-MS [189]. Using a 1:1 water:methanol (v/v) spray solution a variety of PLs could be detected including PG, PE and FFAs. DESI mass spectra were compared to those obtained following ESI-MS analysis of a lipid extract from the same bacteria samples and were found to be similar, although

extraction and analysis by ESI gave an enhanced signal by two-orders of magnitude. Nevertheless, by removing the extraction step the overall analysis time for DESI was significantly reduced. By combining DESI analysis with principal component analysis (PCA) it was shown that the lipid profiles alone were sufficient to not only allow simple differentiation of different bacteria species, but also sub-species. Recently Ferreira *et al*. have extended lipid fingerprinting analyses into the realm of single cells [210]. Single mouse and bovine oocytes were selected and deposited onto glass slides and directly analyzed by DESI-MS. Lipids such as PC, PS, PI, SM and FFAs were readily detected as $[M-H]^-$, $[M+Cl]^-$ or $[M+HCO_2]^-$ ions. Signal enhancement was observed by the addition of 1% formic acid to the spray solution which facilitated the breakdown of the zona pullucida protective layer on the surface of the oocyte, thereby enhancing lipid extraction during the desorption step.

Direct analysis of tissue sections has been widely explored with DESI and the detection of most major lipid classes has been demonstrated (**Table 2**). Analogous to MALDI, direct analysis of tissues sections in positive ion mode detects lipids as $[M+H]^+$, $[M+Na]^+$ and $[M+K]^+$ ions, although the addition of salts or acid to the spray can help ameliorate this effect. Many of the direct tissue studies by DESI have focused on characterizing differences in the lipid profile of diseased and healthy tissue in an attempt to find lipid biomarkers for disease resulting from altered metabolism in the diseased tissue [187, 191-193, 211-213]. Wiseman *et al*. investigated the positive ion lipid profile of metastatic human-liver adenocarcinoma tissue and observed a variety of PC and SM lipids as multiple adducts [187]. The non-tumor region was found to be rich in 16:0-containing phospholipids whereas the transition area between tumor and non-tumor contained significantly more unsaturated PLs. Furthermore, the tumor region had elevated levels of SM (d18:1/16:0), which could suggest a dysfunctional ceramide-mediated apoptosis pathway. Eberlin *et al*. have shown the diagnostic potential of DESI by demonstrating the ability to

distinguish subtypes and histological grades of human brain tumor (oligodendroglioma, astrocytoma, and oligoastrocytoma) [191]. This was accomplished using only the negative ion lipid profile consisting of FFA, PE, PS, PI and ST lipids. Negative ion data was analyzed using multivariate statistical methods and allowed the distinction between tumor sub-type, grade and tumor cell concentration within a given tissue section based on the full-MS profile rather than selected *m/z* channels which is sometimes insufficient for accurate diagnosis [211]. Diagnosis based on DESI-MS was also supported by histological data.

A drawback of tissue analysis by DESI compared to MALDI and SIMS is that the former results in a larger degree of tissue damage. It has been observed for human lens tissue that lipids are only detected when the DESI spray physically disrupted the tissue [185]. It is often desirable to obtain complementary information such as histological data on the same tissue section to allow direct comparison between data sets. However, the disruption of the tissue surface by standard DESI sprays makes this difficult. To overcome this, Eberlin *et al*. [214] described the use of binary solvent systems containing dimethylformamide and either ethanol or acetonitrile that allow acquisition of high quality mass spectral data with minimal tissue damage. These spray solvents have been employed to acquire DESI, MALDI and hematoxylin and eosin staining data on the same tissue section, thus allowing direct correlation of lipid, protein and histological data, respectively [215].

DESI too has been coupled with TLC analysis for the analysis of porcine brain [183] and human lens lipids extracts [184]. In the latter study, TLC/DESI was performed following separation and oxidation of surface exposed unsaturated lipids by ambient ozone (~20 ppb). Upon oxidation each unsaturated lipid yields a low mass aldehyde and hemiacetal ion with a mass characteristic of double bond position. This allows the lipid composition to be probed while also differentially detecting double bond positional isomers. This approach can thus provide complementary information to that obtained by CID that readily reveals headgroup

structure and the length and degree of unsaturation of the fatty acid chains. For example, **Fig. 7a** shows a CID spectrum of [SM (d18:0/24:1)+Na]$^+$ from a human lens lipid extract. The spectrum reveals product ions identifying the phosphocholine headgroup but provides no additional information about the nature of the 24:1 chain. In contrast, analysis by TLC/DESI following exposure to ambient ozone for one hour reveals three sets of ions that allow identification of three distinct double bond isomers of SM (d18:0/24:1) namely, those with double bonds at the *n*-9, *n*-7 and *n*-5 positions (**Fig. 7b**). Identical double bond isomers were also observed for LacCer (d18:0/24:1), suggesting that their presence is an intrinsic property of the ceramide core structure within the human lens. Interestingly, this is the first report of *n*-5 LacCer (d18:0/24:1) in any mammalian tissue. Although the resulting spectra acquired following ozonolysis are complex - with both oxidized and unoxidized lipids present - oxidation products could be assigned to their specific lipid precursor based on their co-localization on the TLC plate. TLC/DESI can also be performed directly on thin tissue sections placed on the TLC plate where the mobile phase extracts and separates lipids in one step, negating the need for off-line extraction. Using this approach Wiseman *et al*. revealed the detection of GLs, STs and PLs separated from a 16 μm rat brain section [194].

4.2 Easy Ambient Sonic Spray Ionization (EASI)

Easy ambient sonic spray ionization (EASI) is based on sonic spray ionization whereby analytes in solution are sprayed from a capillary under the influence of a high-pressure (~30 bar) nebulizing gas without the application of a high voltage [216]. These conditions generate micro-droplets containing an unbalanced charge distribution, that upon solvent vaporization, produce analyte ions identical to those observed with electrospray approaches. EASI directs the sonic-spray (typically 1:1 methanol:water with 0.1% formic

acid or ammonium hydroxide) at the surface where it desorbs/ionizes surface-bound analytes (analogous to DESI). The main advantage of EASI is the simplicity of the source design (with no high voltage) and the production of very clean spectra. However, it does not currently enjoy the popularity of DESI.

With respect to lipid analysis, EASI has been used for TAG and FFA profiling of various vegetable and seed oils deposited onto paper and steel substrates [217-219]. Additionally, PL, TAG and FFA analysis of lipid extracts from hypertriglyceridemic mice spotted onto paper or separated by TLC has been demonstrated [220]. In the latter study, differences in both PL and TAG composition and FFA profiles allowed differentiation of hypertriglyceridemic mice from control mice. Recently, a direct comparison of EASI and DESI for the analysis of rat brain tissue has been provided [221]. Using methanol as the spray solvent both methods produced similar lipid profiles from gray and white brain matter, although DESI produced higher overall ion signal. Furthermore, by comparing ion images acquired using both methods, EASI was suggested to possess a lower dynamic range and be more susceptible to suppression effects. These effects may be attributed to the lower charge density of the EASI generated spray droplets compared to DESI.

Real-time analysis of tissue during ultrasonic surgical aspiration has also been demonstrated by coupling an ultrasonic surgical hand-piece with venturi-EASI (V-EASI) [222]. Tissue debris is collected in the annular water jet then introduced to the V-EASI source where metabolites, lipids and peptides are ionized and detected (**Fig. 8a**). A positive ion spectrum acquired from the cortex of a porcine brain is shown in **Fig. 8b**. Positive ion analysis revealed PC, PE and TAGs, while negative ion analysis allowed the detection of acidic PLs, STs and FFAs. To validate the use of this approach for real-time identification of tumorous tissue during surgery, a variety of healthy and tumorous human brain tissues were analyzed *ex vivo* or post-mortem and the mass spectral data subjected to statistical analysis.

Differentiation of healthy and diseased tissue regions was readily achieved based on altered lipid profiles, highlighting the potential use for diagnosis and real-time surgical feedback. Similar tissue discrimination has been achieved *in vivo* with rapid evaporative ionization mass spectrometry (REIMS) where lipid ionization occurs following tissue via rapid thermal evaporation during electro- or laser-surgery [223].

4.3 Sealing-Surface Sampling Probe (SSSP)

The sealing-surface sampling probe (SSSP) was designed initially for analysis of aluminium backed TLC plates [224]. The device uses a stainless steel plunger with two concentric capillaries and sharpened edges at the bottom of the probe. The inlet capillary is connected to a HPLC pump while the outer capillary is connected to the ionization source. To sample a region of interest the probe is pressed down into the surface with the sharp edges penetrating the surface and forming a tight seal. The extraction solvent flows through the inner capillary onto the surface of interest and extracts analytes that are then carried through the outer capillary to the ionization source, usually ESI, although APCI has been used [225]. Solvent polarity can easily be adjusted to enhance extraction of desired analytes so long as it is compatible with the ionization source used. With modification, the SSSP can also be used on glass backed TLC plates [226].

Most of the applications of the SSSP have involved pharmaceuticals or other small molecules detected from a range of surfaces including TLC plates, tissue sections mounted on adhesive tape and dried blood spots deposited onto filter paper [225] with spatial resolution of 2-4 mm (determined by the probe diameter). Currently there have been limited applications of SSSP for lipid analysis, however in one study GLs from a human brain extract were detected as $[M-H]^-$ ions from a TLC plate [224]. Disadvantages of the SSSP include the

possibility of sample dilution resulting from the continuous solvent flow and the need for washing steps to eliminate carry over between samples. Nonetheless, unlike liquid extraction surface analysis (see section 4.4 below), the SSSP is particularly useful for lipid analysis direct from TLC plates as it does not rely on formation of a liquid microjunction.

4.4 Liquid Extraction Surface Analysis (LESA)

Liquid extraction surface analysis (LESA) extracts surface-bound analytes into a liquid microjunction formed between the sample surface and a droplet dispensed from a conductive pipette tip [227]. The droplet containing extracted analyte is aspirated into the pipette tip and subsequently docked with an automated chip-based nano-ESI source (**Fig. 5b**). This approach is an evolution of the liquid microjunction surface sampling probe technique [228, 229]. Unlike spray-based methods, LESA allows the time in which the solvent droplet is in contact with the surface to be adjusted, thereby giving greater control over the extraction step. A typical LESA experiment uses only several microlitres of solvent and coupling with nano-ESI is advantageous due to its greater sensitivity and for allowing a single microlitre to be analyzed for over 15 minutes. Therefore, unlike methods described earlier, multiple MS and MS/MS spectra (including precursor and neutral loss scans) can be obtained in both polarity modes, providing a comprehensive lipid profile for each sampling region. However, successful LESA requires some compromise in solvent selection between the ability of the solvent to form a stable liquid microjunction on the surface of interest, extract the desired analytes and generate and sustain a stable electrospray. Furthermore, the spatial resolution is determined by the probe diameter, in addition to the solvent and nature of the surface that defines the spread of the pendant droplet. In our experience, when using solvents applicable to lipid analysis the spatial resolution is typically several millimeters.

Despite the infancy of LESA, it has already found success for the analysis of a variety of lipid classes from a range of substrates [230-232]. Stegemann *et al*. have applied LESA to lipid profiling of human atherosclerotic plaques. Using a solvent system of 4:2:1 isopropanol:methanol:chloroform (v/v/v) with 7.5 mM ammonium acetate, 150 lipids were extracted and detected directly from tissue sections. Precursor ion and neutral loss scans were used for selective detection of a range of lipid classes including PE, PS, PC, SM, CE and TAG. Conventional lipid extracts of these tissues were also obtained and analyzed by direct infusion nano-ESI which produced similar spectra. Lipid profiles were compared to those obtained from human plasma and revealed that long chain polyunsaturated cholesterol esters and some SMs were significantly enhanced in plaques. LESA has also been successfully employed for the analysis of lipid deposits on worn contact lenses in an effort to understand the origins of contact lens discomfort and spoilage [231]. Lipid classes detected included PC, SM, cholesterol esters, wax esters and *O*-acyl-ω-hydroxy fatty acids. These studies highlight the ability of LESA to rapidly obtain lipid profiles directly from tissue or polymeric surfaces. However, based on our experience and that of others [233], the solvent system described leads to significant spreading that results in sampling areas extending over several millimeters and limits the ability to profile different regions of a substrate if insufficiently spaced

The detection of lipids from single mammalian cells has also been demonstrated with LESA using class-specific precursor ion MS/MS scans [232]. In this study single cell arrays were prepared by inkjet printing living cells onto a glass microscope slide. The LESA tip was then used to extract and analyze lipids from individual cells present on the surface at pre-defined locations. A variety of PC and SM lipids could be detected from the cells and the corresponding profiles were found to be highly reproducible for each cell type. **Fig. 9** shows a typical LESA spectrum acquired from a single PC12 and L929 cell using a precursor ion

scan of *m/z* 184.1 that provides detection of protonated PC and SM lipids. Furthermore, in combination with PCA analysis, the PC/SM lipid profiles were found to be characteristic and provide differentiation of each of the 3 mammalian cell types analyzed. Cholesterol esters and Cers were also detected following LESA from as little as 50-100 cells. This study highlights the excellent sensitivity of LESA for lipid analysis and its potential to study lipid heterogeneity in cell populations.

Currently, the lower spatial resolution is the greatest disadvantage compared to spray and laser-based approaches and thus more work is still required to develop an approach allowing profiling of tissue sections with greater resolution. Promising results have recently been reported by Laskin *et al* with spatial resolutions as low as 12 µm for lipid imaging from tissue demonstrated using the related nano-DESI technique [234]. Nano-DESI has also been successfully applied to the direct analysis of bacterial colonies on agar substrates [235]. Despite being described as nano-DESI, this technique shares much in common with LESA given that extraction occurs via a liquid microjunction formed between the surface and two capillaries followed by nano-ESI analysis. Additionally, hydrophobic surface treatments are required if one wishes to analyze wettable substrates such as TLC plates that do not facilitate formation of a stable liquid microjunction [236]. Blotting onto hydrophobic surfaces such as PVDF membranes may be one way to overcome this limitation [34, 87]. Nonetheless, LESA is a very promising method for the rapid profiling of lipids from biological tissue and extracts and is likely to be utilized more heavily in the future once its potential is realized.

5. Thermal Desorption and Plasma-Based Methods

Several approaches to direct sampling under ambient conditions have emerged based on the interaction of a heated gas stream or plasma with the surface. Such conditions induce desorption of surface-bound analytes by either direct thermal evaporation or sputtering processes, while ionization of desorbed molecules is typically initiated by mechanisms analogous to those described for APCI [237]. Accordingly, these techniques are best suited for thermally stable, low polarity compounds that are at least semi-volatile. As a result, complex or polar lipid analysis is not well-suited to these techniques, whereas they have found some success for less polar or lower molecular weight species such as TAGs, sterols and various fatty acids. Additionally, analysis is typically performed on extracts or cells and detection of lipids from tissue has yet to be demonstrated for most approaches.

5.1 Atmospheric Pressure Solids Analysis Probe (ASAP)

The atmospheric pressure solids analysis probe (ASAP) consists of a glass probe onto which solid or liquid sample is deposited [238]. As depicted in **Fig. 10a**, analyte desorption occurs upon interaction with a hot nitrogen stream. Ionization follows by APCI mechanisms involving charge and proton exchange with intermediates such as $(H_2O)_nH_3O^+$ and HO^- generated by a nearby corona discharge. Protonated ions are formed with analytes having a gas-phase basicity greater than water and deprotonated ions formed from those with gas-phase acidities greater than water. Advantages of ASAP include simple design and interfacing with many commercial APCI instruments. Indeed dedicated ASAP interfaces are now commercially available on such platforms.

One area where ASAP has found success in lipids analysis has been the study of inhibition of the ergosterol synthesis pathway in fungal cells [239]. Cells were incubated with

inhibition compounds and then directly deposited onto the probe prior to analysis. Using a 300°C gas flow ergosterol and its biosynthetic precursors were detected as molecular radical cations and in some cases de-methylated radicals. By observing the accumulation of intermediates involved in ergosterol production the effect of specific inhibition agents could be deduced. For example, analysis of cells treated with flusilazole resulted in detection of eburicol, suggesting inhibition of the C14-demethylase step. It is important to note that APCI mechanisms are generally more energetic than ESI or MALDI processes which can lead to greater in-source fragmentation of lipids (as evidenced in this study with the observation of de-methylated fragments) [237]. The high desorption temperatures may also result in thermal decomposition prior to ionization.

5.2 Direct Analysis in Real Time (DART)

DART was described in 2005 [14] and along with DESI is one of the most popular ambient ionization approaches. DART begins with the introduction of helium to a glow (or corona) discharge leading to production of electrons, ions and metastable species. Charged components are removed from the gas stream and metastable helium atoms passed through a grid electrode with optional heating. The heated gas then enters the ambient environment and is directed at or above the sample surface near the mass spectrometer inlet. Analyte desorption is likely dominated by thermal evaporation induced by the heated gas stream. Additionally, the use of IR laser desorption coupled with DART has also been described for enhanced resolution (~300 µm) during imaging experiments [240]. While several possible ionization mechanisms have been proposed, the dominant ion forming pathway is believed to occur via interaction of metastable helium with atmospheric components such as water and

oxygen [15]. This produces components such as protonated water clusters and O_2^- which then proton/charge transfer with the analyte.

Lipid analysis using DART has so far been limited to non-polar lipids such as fatty acid methyl esters (FAME), TAGs, cholesterol and cuticular hydrocarbons [241-244]. For example, TAGs have been detected from olive oil desorbed from a glass rod, with a ten-fold increase in signal observed by doping ammonia into the gas stream to facilitate $[M+NH_4]^+$ ion formation [241]. However, desorption/ionization of TAGs resulted in significant fragmentation, a phenomenon not uncommon in DART and one that generally increases with gas temperature [245, 246]. This leads to formation of DAG-like ions with greater abundance than ions arising from intact TAG molecules, thereby reducing sensitivity and making detection of native DAGs difficult. Other applications have demonstrated detection of FAMEs derived from bacterial cells deposited onto a glass capillary in the presence of tetramethylammonium hydroxide [242] and also hydrocarbon-based pheromones from live flies [243]. In the latter study, sampling was performed by gently pressing a steel pin into the surface of the fly and subsequent exposure of the pin to DART. Many unsaturated pheromones were detected as protonated ions and differences observed between virgin males and females and between females before and after courtship. Additionally, the probe also allowed the spatial distribution of pheromones to be investigated simply by sampling different regions of the fly body. For example, the sex pheromone *cis*-vaccenyl acetate is involved in mate partner recognition and was found in much greater abundance on the rear of a male fly than the thorax region. These results provide insight into the molecular signals associated with insect behavior. Similar pheromones have also been observed using direct laser desorption (see above). While TLC analysis is possible with DART, it has not yet been applied to lipids [247]. If accomplished, this can potentially provide an alternate method for detection of non-polar lipids from TLC surfaces. However, the spatial resolution afforded by

the gas flow will be significantly lower than that achieved with laser and spray approaches which may ultimately limit its impact. Nevertheless, the development of hybrid approaches (such as IR laser desorption coupled with DART) may help overcome these limitations.

5.3 Low Temperature Plasma (LTP) Probe

The low temperature plasma (LTP) probe uses a dielectric barrier discharge to generate a "cold" plasma that facilitates desorption/ionization [248]. The plasma is generated upon feeding a discharge gas such as helium, nitrogen or air through the probe and an AC voltage (2.5-5 kV, 2-5 kHz) applied to the outer electrode generating a dielectric barrier discharge. Unlike DART, charged components are not removed prior to surface interaction. The plasma generated components exit the glass tube where they are directed at the sample and exposed to atmospheric components such as oxygen and water, ultimately leading to desorption and ionization of surface-bound analytes that then enter the mass spectrometer [249] (**Fig. 10b**). The desorption mechanisms involved in LTP are still not completely understood but likely involve thermal desorption and chemical sputtering processes. In contrast to DART, the exiting plasma from the LTP probe is ~30°C which minimizes thermal modification of the substrate and results in less thermal decomposition of the analyte [248]. However, this low temperature means some heating of the surface can be required to facilitate sufficient lipid desorption [250].

With respect to lipids, LTP has to-date only been demonstrated for fatty acids. FFAs from olive oil and fatty acid ethyl esters (FAEE) derived from bacterial cells, both of which were deposited onto glass slides, have been detected [251, 252]. In the latter study, FAEEs were detected as protonated ions using a helium discharge gas. FAEE profiles were highly reproducible for different strains of bacteria and also allowed species and sub-species

differentiation. The inherent production of ozone by the dielectric barrier discharge can also be exploited to provide additional structural information for unsaturated fatty acids [250]. This has been shown for FFAs, FAMEs and FAEEs derived from standards and bacterial cells deposited on glass. Ozone reacts with desorbed lipids and produces characteristic aldehydes allowing double bond position(s) to be assigned. **Fig. 11** shows LTP spectra acquired from two 18:1 FAME double bond isomers. Following ozonolysis and ionization aldehydes formed from oxidative cleavage of (a) *n*-11 and (b) *n*-6 double bonds are clearly observed. If not desired, oxidation can be suppressed by covering the probe with a tubular plastic shield and a stream of helium.

While LTP, DART and ASAP are useful methods for fatty acids and TAGs, detection of more complex lipids has yet to be demonstrated. This is likely due to the low volatility of such species making desorption difficult. Furthermore, while using discharge generated ozone is a simple approach for assigning double bond position in fatty acids, it is not as effective for analysis of complex mixtures as the TLC/DESI approach described above, which allows spatially-resolved detection of more complex lipids [184].

5.4 Desorption Atmospheric Pressure Photoionization (DAPPI)

Desorption atmospheric pressure photoionization (DAPPI) uses a microfabricated nebulizing chip to generate a heated vapor jet (~220-350°C), consisting of nitrogen and a doped solvent such as toluene or acetone, to facilitate analyte desorption [253]. The jet is directed at the sample and a DC discharge lamp producing 10 eV photons is positioned above the sample. Analyte desorption occurs mostly by thermal processes, although dissolution into the solvent may also contribute providing some analogy with the mechanisms of DESI (see above). Ionization processes are similar to atmospheric pressure photoionization (APPI)

[253-255] and can involve direct photoionization or charge/proton transfer processes with photoactivated dopants. Thermally insulating materials such as PTFE and poly(methyl methacrylate) have been found to be the most effective substrates, although detection has been achieved from a range of surfaces [254].

Like the aforementioned plasma and thermal desorption methods, DAPPI is best suited for non-polar compounds not easily ionized by electrospray methods. Nevertheless, a variety of lipid classes have been detected with varying success. Suni *et al*. compared analysis of fatty acids, vitamins, sterols and PLs by DESI and DAPPI from Teflon substrates [202]. DAPPI gave a ten-fold increase in sensitivity for FFAs and vitamins E and K1, highlighting the suitability for non-polar analytes. By contrast, DAPPI was less suited for analysis of larger and more polar lipids such as TAGs and PLs that required higher desorption temperatures resulting in extensive fragmentation. For example, DAPPI spectra of PLs revealed extensive headgroup losses and, for some classes, ions corresponding to the intact lipids were completely absent. In contrast to other thermal and plasma-based techniques discussed in this section, DAPPI has been applied to direct tissue analysis [256]. This was achieved by analyzing a rat brain section with acetone as the dopant and resulted almost exclusively in an intense signal corresponding to the $[M+H-H_2O]^+$ ion of cholesterol with more than 100 times greater signal than observed with DESI on the same instrument. Along with the enhanced ionization efficiency for non-polar lipids, another possible contributor to this enhanced signal is the larger desorption area of DAPPI (*ca*. 1 mm) compared to DESI (200-500 μm). This could potentially provide more analyte for ionization and analysis from a given sampling region. This larger desorption area however, makes DAPPI less suitable for imaging applications.. Although DAPPI was unable to detect additional lipid classes from tissue such as PLs and sphingolipids detected by DESI, it serves to highlight the suitability of DAPPI for non-polar lipids that are difficult to observe with spray-based approaches.

Furthermore, the recent coupling of IR-laser ablation with APPI has been shown to provide improved spatial resolution (~300 µm) compared to DAPPI, thereby enhancing the suitability of APPI-based approaches for imaging applications [257].

6. Alternative Approaches

6.1 Probe Electrospray Ionization (PESI)

Probe electrospray ionization (PESI) employs a steel needle with a small diameter tip mounted to a motorized stage [258]. The sharp tip is pressed down into the sample (such as solution or a tissue section) leading to the adhesion of several picolitres of liquid and/or surface material to the tip. The tip is lifted from the sample and moved towards to mass spectrometer inlet where a high voltage (2-3 kV) is applied to the needle inducing an electrospray (**Fig. 12a**). The small volumes produce nano-ESI type ionization and therefore little fragmentation is observed. Direct analysis of the droplet avoids some of the problems associated with undissolved material blocking nano-ESI capillaries. This is a crucial property if one wishes to sample material removed directly from a surface where the risks of contamination are heightened.

Lipid analysis by PESI has so far been accomplished from direct tissue sampling, including analysis of live mice [259, 260]. Tissue analysis however, can pose a challenge if it does not contain sufficient water (or other solvent) to produce an electrospray. One way to overcome this is by using an auxiliary sprayer to spray water or organic solvent vapor onto the probe where it condenses and facilitates a stable electrospray [261]. Lipids detected from tissue sections include PC, PS, PI, GalCer and TAGs [259, 261, 262]. TAGs were detected as ammonium adducts by doping the auxiliary spray (7:3 MeOH:$CHCl_3$ v/v) with ammonium

acetate [259], while other lipids detected as positive ions (PC, GalCer) could be observed as multiple adducts due to endogenous salts: a feature common to many of the methods described herein. Yoshimura *et al*. described the lipid analysis of live, anesthetized mice both with and without induced steatosis [259]. Liver tissue was exposed by laparotomy and directly analyzed by PESI. The PESI-MS spectra acquired from control mice without steatosis were dominated by PC lipids, whereas analysis of steatotic mice revealed much higher signal for TAG molecules. Analysis of tumorous and healthy tissues sections by PESI also allowed their differentiation based on the corresponding lipid profiles [259]. PESI can also facilitate imaging with the spatial resolution determined by the diameter of the needle tip. This has been demonstrated for PC and GalCer lipids in mouse brain sections where a spatial resolution of ~60 µm was achieved which is comparable to laser-based methods [261].

One difficulty encountered with PESI is carry-over due to the incomplete removal of material from the probe during ionization [260]. Although washing steps can be employed in between samples [261], complete removal of material could require several washes with different solvents which necessarily increases analysis time. Nonetheless, the high sensitivity and salt tolerance of PESI makes it well suited for rapid, direct lipid analysis from tissue surfaces. Furthermore, preliminary results on porcine retina tissue suggest PESI may allow depth profiling of lipids in tissue sections, whereby increasing penetration of the needle into the tissue may reveal changes in the lipid composition as a function of depth [261]. It is also conceivable that the small probe diameter could allow analysis and extraction at the single cell level in a manner similar to that described by Masujima [263].

6.2 Paper Spray Ionization (PSI)

Paper spray ionization (PSI) is perhaps the simplest of all surface-based mass spectrometry techniques. It uses a paper substrate cut into a triangle onto which a high voltage (2-5 kV) is applied as it is held ~5 mm from the MS inlet [264]. The sample is typically applied to the paper by either deposition from solution or simply wiping the paper onto the surface of interest. Solvents added to the paper (typically methanol or methanol:water mixtures) then migrate with the analytes towards the tip where they are ionized by the high electric field (**Fig 12b**). The ionization process has been compared to nano-electrospray, although PSI requires higher spray voltages and produces ions with slightly lower internal energies [265]. Unlike conventional ESI methods, PSI can also be carried out using non-polar solvents such as pentane/hexane with the advantage of allowing analysis of solid analytes insoluble in conventional solvent systems. For example, cholesterol sulfate and PC standards have been detected by addition of hexane to the paper [266].

Given its infancy, lipid applications of PSI have so far been limited. Most applications of PSI are focused on clinical applications, such as drugs and dried blood spots [264, 267], although some success has been demonstrated for lipid analysis. For example, lipids can be detected directly from tissue [268]. This is accomplished by punching out a ~1 mm^3 region of tissue and placing it onto the paper substrate with subsequent solvent deposition. The solvent extracts lipids that are then carried towards the paper tip and ionized. Several tissues including tumorous and healthy human prostate tissue and rat brain have been analyzed with this approach and allowed detection of PC and SM in positive ion mode and PS, PG, ST and Cer in negative ion mode. Distinct positive ion lipid profiles were observed in tumorous and healthy prostate tissue allowing the two types to be distinguished. For example, an increase in the $[M+K]^+$ ion intensity of PC (34:1) and decreased levels of SM (34:1) were observed in tumorous tissue. Thus this simple approach can rapidly acquire lipid profiles from different

tissue regions and may find use as a means to support imaging data or identify lipids of interest for more targeted analysis (*e.g.*, accurate mass or MS/MS). Some lipids not easily ionized by electrospray can be subjected to *in situ* derivatization by spiking the paper substrate with a suitable reagent. An example of this is the detection of cholesterol from human serum by spiking the paper with betaine aldehyde, analogous to the reactive DESI approach [264]. Reactive-PSI methods have the potential to further enhance the range of compounds detectable with this approach.

6.3 Laser-Induced Acoustic Desorption (LIAD)

Laser-induced acoustic desorption (LIAD) uses an acoustic wave generated by a laser pulse to desorb analytes from a surface. LIAD directs the laser at the rear side of a substrate (usually a metal foil) containing solid or liquid analyte on the front side. The laser induces a shockwave that travels through the substrate and desorbs material via mechanical forces with little dissociation. The size of the ablated area has been reported to be several millimeters in diameter [269]. Desorbed analytes are then ionized by subsequent interaction with the ion source. A variety of ionization techniques have been coupled with LIAD including chemical ionization [270], ESI [271] and APCI [272]. This desorption mechanism is not dependant on laser absorption by the analyte and is suitable for analysis of thermally labile and non-volatile analytes. TLC analysis is also possible by placing a developed TLC plate onto a glass slide and incorporating a thin glycerol film between TLC plate and glass slide. This is necessary to initiate adequate desorption from the TLC plate, although it leads to noticeable desorption of silica from the surface which may cause contamination [269]. In terms of lipids, LIAD has so far only been used for non-polar lipids such as sterols and other hydrocarbons [270, 272,

273]. In a study by Jin *et al*. eight steroids, squalene and β-carotene were successfully analyzed using a combination of LIAD with chemical ionization, APCI and ESI, [273].

LIAD does not enjoy the popularity of other surface analysis approaches, despite it allowing desorption of a wide range of analytes. Although only non-polar lipids have been analyzed to date, other intact biomolecules such as peptides and proteins have been detected [271], suggesting LIAD will also be suitable for the analysis of additional lipid classes. Furthermore, the suitability of the acoustic desorption mechanism for many different molecular classes, combined with the ability to interface with a variety of ionization sources, can provide analytical access to a wider range of analytes than conventional spray and laser-based techniques alone.

7. Conclusions

As evident from the preceding discussion there are now many approaches available that allow the direct detection of lipids from surfaces commonly encountered in lipid analysis. Although no single technique is best suited to all applications, a number of these approaches have particular advantages for direct analysis of biological tissue and are also well suited for characterization of lipids derived from biological extracts and intact cells (including single cells). Several of the methods described can also be directly coupled to additional analytical protocols, such as TLC. Direct TLC analysis by these approaches offers advantages over conventional staining techniques, which provide little molecular information on individual lipids present on the plate.

Currently, the ability of MALDI and DESI to detect most major lipid classes from a variety of surfaces makes these the methods of choice in the majority of cases. Although the

typical spatial resolution of DESI (200-500 μm) and MALDI (25-100 μm) does not allow the sub-cellular resolution afforded by SIMS, all have found success in imaging studies. While increasingly high-resolution imaging capabilities are desired, it must be remembered that this comes at the cost of increased analysis time and requires greater mass spectrometric sensitivity due to the production of fewer ions per pixel. In many applications however, high spatial resolution is not a necessity (*i.e.*, analysis of extracts, TLC plates and non-imaging studies) and the typical resolution afforded by these commercially available technologies is sufficient. Nonetheless, improving the achievable resolution of these methods is an active area of research.

While MALDI, SIMS and DESI have been the dominant techniques employed to date, we envisage several emerging techniques to play a greater role in the future. Specifically, NIMS and NALDI can provide enhanced sensitivity relative to MALDI without a matrix and should become more widespread as suitable substrates become more widely available. Similarly IR-laser-based techniques (*e.g.*, IR-MALDI and LAESI), given their suitability for TLC plate analysis and direct sampling of water-rich samples, including tissue sections, show much promise. Indeed the recent commercialization of LAESI is likely to stimulate a rapid expansion in this area. Finally, although in its infancy, LESA is a promising approach for the rapid lipid profiling of biological tissue as it affords greater control over the extraction and ionization steps than other spray-based methods. Although it typically achieves lower spatial resolution, LESA provides a prolonged and stable signal from each sampling region on the surface and thus allows for acquisition of multiple MS, MS/MS and even high resolution spectra. This greatly enhances the range of lipids detected and structural information obtained from a single spot.

By providing capabilities that allow lipid analysis directly from relevant surfaces with minimal sample manipulation, along with the acquisition of spatially resolved information, the methods described here should be viewed as providing complementary information to conventional (extraction-based) lipid analysis. However, several challenges still need to be addressed. For example, ion suppression is a factor in all mass spectrometry methods, but becomes more significant with increasing sample complexity (such as that encountered when sample preparation is minimized). As a result, all lipids present in a complex sample are unlikely to be detected in a single direct analysis and one must be aware of the fact that additional lipids that are present may not have been detected. In such instances, direct coupling of surface analysis with prior TLC separation can go a long way to reduce these effects. Additionally, in the case of direct tissue and cell analysis, the inability to pre-concentrate analytes means their localized surface concentration must be sufficient to allow detection. This can become a limiting factor when either the desired target area is small (*i.e.*, a high spatial resolution is required) and/or the target lipid(s) are of low abundance (such as lipids typically involved in signaling pathways). Finally, quantitative analysis is essential in many lipidomic workflows but development of robust and accurate quantitative methods for the techniques described here, particularly for tissue analysis, has been particularly challenging. This is largely due to ion suppression effects, the possibility of different desorption efficiencies from different tissue regions and, in the case of MALDI, the need for (and difficulty in obtaining) a perfectly homogenous matrix coating. As a result there are few reports of quantitative lipid analysis using the surface analysis methods described herein. Nevertheless, the development of quantitative protocols is an important area of ongoing research. For example, by applying a PC lipid internal standard either on top of or below the tissue section prior to matrix application, relative quantitation of PC lipids from nerve tissue has been demonstrated [274]. Such developments are essential if one wishes to acquire

quantitative information for lipids from tissue. Although not yet applied to lipids, PSI has also shown quantitative capabilities by doping the paper or sample with an internal standard [275]; such approaches may allow the rapid quantitation of lipid extracts and possible even tissues. Furthermore, it is possible that liquid extraction and spray-based approaches will find success for relative quantitation due to the ease in which internal standards may be added to the extraction or spray solvent [276], although to our knowledge this has yet to be reported for lipid analysis. The lack of current quantitative approaches perhaps represents the greatest challenge currently facing direct surface analysis methods if they are to find more wide-spread incorporation into lipidomic investigations.

Acknowledgments

S.R.E. is supported by an Australian Postgraduate Award. S.J.B. acknowledges research funding from the ARC Centre of Excellence for Free Radical Chemistry and Biotechnology (CE0561607). T.W.M. and S.J.B. are grateful for funding through the ARC Discovery Program (DP120102922). T.W.M. and M .in het P. are supported by fellowships from the Australian Research Council (FT110100249 and FT0990846, respectively).

References

[1] Wenk MR. Lipidomics: New tools and applications. Cell. 2010;143:888-95.
[2] Wenk MR. The emerging field of lipidomics. Nat Rev Drug Discov. 2005;4:594-610.
[3] van Meer G. Cellular lipidomics. EMBO J. 2005;24:3159-65.
[4] Yetukuri L, Ekroos K, Vidal-Puig A, Oresic M. Informatics and computational strategies for the study of lipids. Mol Biosyst. 2008;4:121-7.
[5] Fenn JB, Mann M, Meng CK, Wong SF, Whitehouse CM. Electrospray ionization for mass spectrometry of large biomolecules. Science. 1989;246:64-71.
[6] Pulfer M, Murphy RC. Electrospray mass spectrometry of phospholipids. Mass Spectrom Rev. 2003;22:332-64.
[7] Han X, Gross RW. Structural determination of picomole amounts of phospholipids via electrospray ionization tandem mass spectrometry. J Am Soc Mass Spectrom. 1995;6:1202-10.
[8] Blanksby SJ, Mitchell TW. Advances in mass spectrometry for lipidomics. Annu Rev Anal Chem. 2010;3:433-65.
[9] Fuchs B, Süß R, Teuber K, Eibisch M, Schiller J. Lipid analysis by thin-layer chromatography--a review of the current state. J Chromatogr A. 2011;1218:2754-74.
[10] Karas M, Hillenkamp F. Laser desorption ionization of proteins with molecular masses exceeding 10,000 daltons. Anal Chem. 1988;60:2299-301.
[11] Tanaka K, Waki H, Ido Y, Akita S, Yoshida Y, Yoshida T, et al. Protein and polymer analyses up to m/z 100 000 by laser ionization time-of-flight mass spectrometry. Rapid Commun Mass Spectrom. 1988;2:151-3.
[12] Werner HW. The use of secondary ion mass spectrometry in surface analysis. Surf Sci. 1975;47:301-23.
[13] Zoltan T, Justin. M W, Bodgan G, Cooks RG. Mass spectrometry sampling under ambient conditions with desorption electrospray ionization. Science. 2004;306:471-3.
[14] Cody RB, Laramee JA, Durst HD. Versatile new ion source for the analysis of materials in open air under ambient conditions. Anal Chem. 2005;77:2297-302.
[15] Harris GA, Galhena AS, Fernandez FM. Ambient sampling/ionization mass spectrometry: Applications and current trends. Anal Chem. 2011;83:4508-38.
[16] Van Berkel GJ, Pasilis SP, Ovchinnikova O. Established and emerging atmospheric pressure surface sampling/ionization techniques for mass spectrometry. J Mass Spectrom. 2008;43:1161-80.
[17] Huang M-Z, Yuan C-H, Cheng S-C, Cho Y-T, Shiea J. Ambient ionization mass spectrometry. Annu Rev Anal Chem. 2010;3:43-65.
[18] Fuchs B, Süß R, Schiller J. An update of MALDI-TOF mass spectrometry in lipid research. Prog Lipid Res. 2010;49:450-75.
[19] Zemski Berry KA, Hankin JA, Barkley RM, Spraggins JM, Caprioli RM, Murphy RC. MALDI imaging of lipid biochemistry in tissues by mass spectrometry. Chem Rev. 2011;111:6491-512.
[20] Eberlin LS, Ferreira CR, Dill AL, Ifa DR, Cooks RG. Desorption electrospray ionization mass spectrometry for lipid characterization and biological tissue imaging. Biochim Biophys Acta, Mol Cell Biol Lipids. 2011;1811:946-60.
[21] Passarelli MK, Winograd N. Lipid imaging with time-of-flight secondary ion mass spectrometry (ToF-SIMS). Biochim Biophys Acta, Mol Cell Biol Lipids. 2011;1811:976-90.
[22] Karas M, Bachmann D, Hillenkamp F. Influence of the wavelength in high-irradiance ultraviolet laser desorption mass spectrometry of organic molecules. Anal Chem. 1985;57:2935-9.

[23] Karas M, Bachmann D, Bahr U, Hillenkamp F. Matrix-assisted ultraviolet laser desorption of non-volatile compounds. Int J Mass Spectrom Ion Process. 1987;78:53-68.
[24] van den Brink OF, Boon JJ, O'Connor PB, Duursma MC, Heeren RMA. Matrix-assisted laser desorption/ionization fourier transform mass spectrometric analysis of oxygenated triglycerides and phosphatidylcholines in egg tempera paint dosimeters used for environmental monitoring of museum display conditions. J Mass Spectrom. 2001;36:479-92.
[25] Kaletaş BK, van der Wiel IM, Stauber J, Lennard JD, Güzel C, Kros JM, et al. Sample preparation issues for tissue imaging by imaging MS. Proteomics. 2009;9:2622-33.
[26] Hankin JA, Barkley RM, Murphy RC. Sublimation as a method of matrix application for mass spectrometric imaging. J Am Soc Mass Spectrom. 2007;18:1646-52.
[27] Murphy RC, Hankin JA, Barkley RM, Zemski Berry KA. MALDI imaging of lipids after matrix sublimation/deposition. Biochim Biophys Acta, Mol Cell Biol Lipids. 2011;1811:970-5.
[28] Amstalden van Hove ER, Smith DF, Heeren RMA. A concise review of mass spectrometry imaging. J Chromatogr A. 2010;1217:3946-54.
[29] Touboul D, Brunelle A, Laprevote O. Mass spectrometry imaging: Towards a lipid microscope? Biochimie. 2011;93:113-9.
[30] Vidova V, Pol J, Volny M, Novak P, Havlicek V, Wiedmer SK, et al. Visualizing spatial lipid distribution in porcine lens by MALDI imaging high-resolution mass spectrometry. J Lipid Res. 2010;51:2295-302.
[31] Thomas A, Charbonneau JL, Fournaise E, Chaurand P. Sublimation of new matrix candidates for high spatial resolution imaging mass spectrometry of lipids: Enhanced information in both positive and negative polarities after 1,5-diaminonapthalene deposition. Anal Chem. 2012;84:2048-54.
[32] Jackson S, Wang H-Y, Woods A. In situ structural characterization of phosphatidylcholines in brain tissue using MALDI-MS/MS. J Am Soc Mass Spectrom. 2005;16:2052-6.
[33] Schiller J, Süß R, Fuchs B, Müller M, Petković M, Zschörnig O, et al. The suitability of different DHB isomers as matrices for the MALDI-TOF MS analysis of phospholipids: Which isomer for what purpose? Eur Biophys J. 2007;36:517-27.
[34] Goto-Inoue N, Hayasaka T, Taki T, Gonzalez TV, Setou M. A new lipidomics approach by thin-layer chromatography-blot-matrix-assisted laser desorption/ionization imaging mass spectrometry for analyzing detailed patterns of phospholipid molecular species. J Chromatogr A. 2009;1216:7096-101.
[35] Teuber K, Schiller J, Fuchs B, Karas M, Jaskolla TW. Significant sensitivity improvements by matrix optimization: A MALDI-TOF mass spectrometric study of lipids from hen egg yolk. Chem Phys Lipids. 2010;163:552-60.
[36] Le CH, Han J, Borchers CH. Dithranol as a MALDI matrix for tissue imaging of lipids by fourier transform ion cyclotron resonance mass spectrometry. Anal Chem. 2012;84:8391-8.
- , Giralt MaT, et al. Profiling and imaging of lipids on brain and liver tissue by matrix-assisted laser desorption/ionization mass spectrometry using 2-mercaptobenzothiazole as a matrix. Anal Chem. 2008;80:9105-14.
[38] Veloso A, Astigarraga E, Barreda-Gómez G, Manuel I, Ferrer I, Teresa Giralt M, et al. Anatomical distribution of lipids in human brain cortex by imaging mass spectrometry. J Am Soc Mass Spectrom. 2011;22:329-38.
[39] Estrada R, Puppato A, Borchman D, Yappert MC. Reevaluation of the phospholipid composition in membranes of adult human lenses by ^{31}P NMR and MALDI MS. Biochim Biophys Acta, Biomembr. 2010;1798:303-11.

[40] Rujoi M, Estrada R, Yappert MC. In situ MALDI-TOF MS regional analysis of neutral phospholipids in lens tissue. Anal Chem. 2004;76:1657-63.
[41] Stübiger G, Belgacem O. Analysis of lipids using 2,4,6-trihydroxyacetophenone as a matrix for MALDI mass spectrometry. Anal Chem. 2007;79:3206-13.
[42] Urban PL, Chang C-H, Wu J-T, Chen Y-C. Microscale MALDI imaging of outer-layer lipids in intact egg chambers from drosophila melanogaster. Anal Chem. 2011;83:3918-25.
[43] Sun G, Yang K, Zhao Z, Guan S, Han X, Gross RW. Matrix-assisted laser desorption/ionization time-of-flight mass spectrometric analysis of cellular glycerophospholipids enabled by multiplexed solvent dependent analyte−matrix interactions. Anal Chem. 2008;80:7576-85.
[44] Wang H-Y, Jackson S, Woods A. Direct MALDI-MS analysis of cardiolipin from rat organs sections. J Am Soc Mass Spectrom. 2007;18:567-77.
[45] Fuchs B, Schiller J, Süß R, Zscharnack M, Bader A, Müller P, et al. Analysis of stem cell lipids by offline HPTLC-MALDI-TOF MS. Anal Bioanal Chem. 2008;392:849-60.
[46] Calvano CD, Zambonin CG, Palmisano F. Lipid fingerprinting of gram-positive lactobacilli by intact cells – matrix-assisted laser desorption/ionization mass spectrometry using a proton sponge based matrix. Rapid Commun Mass Spectrom. 2011;25:1757-64.
[47] Calvano C, Carulli S, Palmisano F. 1h-pteridine-2,4-dione (lumazine): A new MALDI matrix for complex (phospho)lipid mixtures analysis. Anal Bioanal Chem. 2010;398:499-507.
[48] Jackson SN, Woods AS. Direct profiling of tissue lipids by MALDI-TOFMS. J Chromatogr B. 2009;877:2822-9.
[49] Estrada R, Yappert MC. Alternative approaches for the detection of various phospholipid classes by matrix-assisted laser desorption/ionization time-of-flight mass spectrometry. J Mass Spectrom. 2004;39:412-22.
[50] Cerruti CD, Benabdellah F, Laprévote O, Touboul D, Brunelle A. MALDI imaging and structural analysis of rat brain lipid negative ions with 9-aminoacridine matrix. Anal Chem. 2012;84:2164-71.
[51] Marsching C, Eckhardt M, Gröne H-J, Sandhoff R, Hopf C. Imaging of complex sulfatides SM3 and SB1a in mouse kidney using MALDI-TOF/TOF mass spectrometry. Anal Bioanal Chem. 2011;401:53-64.
[52] Cheng H, Sun G, Yang K, Gross RW, Han X. Selective desorption/ionization of sulfatides by MALDI-MS facilitated using 9-aminoacridine as matrix. J Lipid Res. 2010;51:1599-609.
[53] Kyogashima M, Tamiya-Koizumi K, Ehara T, Li G, Hu R, Hara A, et al. Rapid demonstration of diversity of sulfatide molecular species from biological materials by MALDI-TOF MS. Glycobiology. 2006;16:719-28.
[54] Deeley. J. M., Hankin JA, Friedrich MC, Murphy RC, Truscott RJW, Blanksby. S. J., et al. Sphingolipid distribution changes with age in the human lens. J Lipid Res. 2010;51:2753.
[55] Suzuki Y, Suzuki M, Ito E, Goto-Inoue N, Miseki K, Lida J, et al. Convenient structural analysis of glycosphingolipids using MALDI-QIT-TOF mass spectrometry with increased laser power and cooling gas flow. J Biochem. 2006;139:771-7.
[56] Asbury G, Al-Saad K, Siems W, Hannan R, Hill H. Analysis of triacylglycerols and whole oils by matrix-assisted laser desorption/ionization time of flight mass spectrometry. J Am Soc Mass Spectrom. 1999;10:983-91.
[57] Benard S, Arnhold J, Lehnert M, Schiller J, Arnold K. Experiments towards quantification of saturated and polyunsaturated diacylglycerols by matrix-assisted laser desorption and ionization time-of-flight mass spectrometry. Chem Phys Lipids. 1999;100:115-25.

[58] Ferreira CR, Saraiva SA, Catharino RR, Garcia JS, Gozzo FC, Sanvido GB, et al. Single embryo and oocyte lipid fingerprinting by mass spectrometry. J Lipid Res. 2010;51:1218-27.
[59] Guyon F, Absalon C, Eloy A, Salagoity MH, Esclapez M, Medina B. Comparative study of matrix-assisted laser desorption/ionization and gas chromatography for quantitative determination of cocoa butter and cocoa butter equivalent triacylglycerol composition. Rapid Commun Mass Spectrom. 2003;17:2317-22.
[60] Hidaka H, Hanyu N, Sugano M, Kawasaki K, Yamauchi K, Katsuyama T. Analysis of human serum lipoprotein lipid composition using MALDI-TOF mass spectrometry. Annals of Clinical & Laboratory Science. 2007;37:213-21.
[61] Sherrod SD, Diaz AJ, Russell WK, Cremer PS, Russell DH. Silver nanoparticles as selective ionization probes for analysis of olefins by mass spectrometry. Anal Chem. 2008;80:6796-9.
[62] Perdian DC, Cha S, Oh J, Sakaguchi DS, Yeung ES, Lee YJ. In situ probing of cholesterol in astrocytes at the single-cell level using laser desorption ionization mass spectrometric imaging with colloidal silver. Rapid Commun Mass Spectrom. 2010;24:1147-54.
[63] Zschörnig O, Pietsch M, Süß R, Schiller J, Gütschow M. Cholesterol esterase action on human high density lipoproteins and inhibition studies: Detection by MALDI-TOF MS. J Lipid Res. 2005;46:803-11.
[64] Schiller J, Zschörnig O, Petkovic´ M, Müller M, Arnhold J, Arnold K. Lipid analysis of human HDL and LDL by MALDI-TOF mass spectrometry and 31P-NMR. J Lipid Res. 2001;42:1501-8.
[65] Shroff R, Svatoš A. 1,8-bis(dimethylamino)naphthalene: A novel superbasic matrix for matrix-assisted laser desorption/ionization time-of-flight mass spectrometric analysis of fatty acids. Rapid Commun Mass Spectrom. 2009;23:2380-2.
[66] Shroff R, Rulíšek L, Doubský J, Svatoš A. Acid–base-driven matrix-assisted mass spectrometry for targeted metabolomics. Proc Nat Acad Sci. 2009;106:10092-6.
[67] Liu Y, Liu J, Deng C, Zhang X. Graphene and graphene oxide: Two ideal choices for the enrichment and ionization of long-chain fatty acids free from matrix-assisted laser desorption/ionization matrix interference. Rapid Commun Mass Spectrom. 2011;25:3223-34.
[68] Yu H, Lopez E, Young SW, Luo J, Tian H, Cao P. Quantitative analysis of free fatty acids in rat plasma using matrix-assisted laser desorption/ionization time-of-flight mass spectrometry with meso-tetrakis porphyrin as matrix. Anal Biochem. 2006;354:182-91.
[69] Ayorinde FO, Garvin K, Saeed K. Determination of the fatty acid composition of saponified vegetable oils using matrix-assisted laser desorption/ionization time-of-flight mass spectrometry. Rapid Commun Mass Spectrom. 2000;14:608-15.
[70] Hayasaka T, Goto-Inoue N, Zaima N, Shrivas K, Kashiwagi Y, Yamamoto M, et al. Imaging mass spectrometry with silver nanoparticles reveals the distribution of fatty acids in mouse retinal sections. J Am Soc Mass Spectrom. 2010;21:1446-54.
[71] Trimpin S, Clemmer D, McEwen C. Charge-remote fragmentation of lithiated fatty acids on a TOF-TOF instrument using matrix-ionization. J Am Soc Mass Spectrom. 2007;18:1967-72.
[72] Goto-Inoue N, Hayasaka T, Zaima N, Setou M. Imaging mass spectrometry for lipidomics. Biochim Biophys Acta, Mol Cell Biol Lipids. 2011;1811:961-9.
[73] Schiller J, Süss R, Arnhold J, Müller M, Petković M, Spalteholz H, et al. Matrix-assisted laser desorption and ionization time-of-flight (MALDI-TOF) mass spectrometry in lipid and phospholipid research. Prog Lipid Res. 2004;43:449-88.
[74] Fuchs B, Schiller J. Application of MALDI-TOF mass spectrometry in lipidomics. Eur J Lipid Sci Technol. 2009;111:83-98.

[75] Murphy RC, Hankin JA, Barkley RM. Imaging of lipid species by MALDI mass spectrometry. J Lipid Res. 2009;50:S217-322.
[76] Cerruti C, Touboul D, Guérineau V, Petit V, Laprévote O, Brunelle A. MALDI imaging mass spectrometry of lipids by adding lithium salts to the matrix solution. Anal Bioanal Chem. 2011;401:75-87.
[77] Wang H-YJ, Liu CB, Wu H-W. A simple desalting method for direct MALDI mass spectrometry profiling of tissue lipids. J Lipid Res. 2011;52:840-9.
[78] Petkovic M, Schiller J, Müller M, Benard S, Reichl S, Arnold K, et al. Detection of individual phospholipids in lipid mixtures by matrix-assisted laser desorption/ionization time-of-flight mass spectrometry: Phosphatidylcholine prevents the detection of further species. Anal Biochem. 2001;289:202-16.
[79] Fuchs B, Schiller J, Süß R, Nimptsch A, Schürenberg M, Suckau D. Capabilities and disadvantages of combined matrix-assisted laser-desorption/ionization time-of-flight mass spectrometry (MALDI-TOF MS) and high-performance thin-layer chromatography (HPTLC): Analysis of egg yolk lipids. J Planar Chromatogr - Mod TLC. 2009;22:35-42.
[80] Johanson RA, Buccafusca R, Quong JN, Shaw MA, Berry GT. Phosphatidylcholine removal from brain lipid extracts expands lipid detection and enhances phosphoinositide quantification by matrix-assisted laser desorption/ionization time-of-flight (MALDI-TOF) mass spectrometry. Anal Biochem. 2007;362:155-67.
[81] Fuchs B, Nimptsch A, Schiller J, Süss R. Analysis of brain lipids by directly coupled matrix-assisted laser desorption ionization time-of-flight mass spectrometry and high-performance thin-layer chromatography. J AOAC Int. 2008;91:1227-35.
[82] Fuchs B, Süß R, Nimptsch A, Schiller J. MALDI-TOF-MS directly combined with TLC: A review of the current state. Chromatographia. 2009;69:95-105.
[83] Muthing J, Distler U. Advances on the compositional analysis of glycosphingolipids combining thin-layer chromatography with mass spectrometry. Mass Spectrom Rev. 2010;29:425-79.
[84] Schiller J, Müller K, Süss R, Arnhold J, Gey C, Herrmann A, et al. Analysis of the lipid composition of bull spermatozoa by MALDI-TOF mass spectrometry-a cautionary note. Chem Phys Lipids. 2003;126:85-94.
[85] Vieler A, Wilhelm C, Goss R, Süss R, Schiller J. The lipid composition of the unicellular green alga chlamydomonas reinhardtii and the diatom cyclotella meneghiniana investigated by MALDI-TOF MS and TLC. Chem Phys Lipids. 2007;150:143-55.
[86] Cohen SL. Ozone in ambient air as a source of adventitious oxidation. A mass spectrometric study. Anal Chem. 2006;78:4352-62.
[87] Goto-Inoue N, Hayasaka T, Sugiura Y, Taki T, Li Y-T, Matsumoto M, et al. High-sensitivity analysis of glycosphingolipids by matrix-assisted laser desorption/ionization quadrupole ion trap time-of-flight imaging mass spectrometry on transfer membranes. J Chromatogr B. 2008;870:74-83.
[88] Jackson S, Ugarov M, Post J, Egan T, Langlais D, Schultz J, et al. A study of phospholipids by ion mobility TOFMS. J Am Soc Mass Spectrom. 2008;19:1655-62.
[89] Jackson SN, Ugarov M, Egan T, Post JD, Langlais D, Albert Schultz J, et al. MALDI-ion mobility-TOFMS imaging of lipids in rat brain tissue. J Mass Spectrom. 2007;42:1093-8.
[90] McLean JA, Ridenour WB, Caprioli RM. Profiling and imaging of tissues by imaging ion mobility-mass spectrometry. J Mass Spectrom. 2007;42:1099-105.
[91] Jackson SN, Colsch B, Egan T, Lewis EK, Schultz JA, Woods AS. Gangliosides' analysis by MALDI-ion mobility MS. Analyst. 2011;136:463-6.
[92] Shanta SR, Zhou L-H, Park YS, Kim YH, Kim Y, Kim KP. Binary matrix for MALDI imaging mass spectrometry of phospholipids in both ion modes. Anal Chem. 2011;83:1252-9.

[93] Laiko VV, Baldwin MA, Burlingame AL. Atmospheric pressure matrix-assisted laser desorption/ionization mass spectrometry. Anal Chem. 2000;72:652-7.
[94] Creaser CS, Ratcliffe L. Atmospheric pressure matrix-assisted laser desorption/ionisation mass spectrometry: A review. Curr Anal Chem. 2006;2:9-15.
[95] Tan PV, Laiko VV, Doroshenko VM. Atmospheric pressure MALDI with pulsed dynamic focusing for high-efficiency transmission of ions into a mass spectrometer. Anal Chem. 2004;76:2462-9.
[96] Trimpin S, Herath TN, Inutan ED, Cernat SA, Miller JB, Mackie K, et al. Field-free transmission geometry atmospheric pressure matrix-assisted laser desorption/ionization for rapid analysis of unadulterated tissue samples. Rapid Commun Mass Spectrom. 2009;23:3023-7.
[97] Roy MC, Nakanishi H, Takahashi K, Nakanishi S, Kajihara S, Hayasaka T, et al. Salamander retina phospholipids and their localization by MALDI imaging mass spectrometry at cellular size resolution. J Lipid Res. 2012;52:463-70.
[98] Ito E, Tominaga A, Waki H, Miseki K, Tomioka A, Nakajima K, et al. Structural chracterization of monosialo-, disialo- and trisialo-gangliosides by negative ion AP-MALDI-QIT-TOF mass spectrometry with MSn switching. Neurochem Res. 2012:1-10.
[99] Perdian DC, Schieffer GM, Houk RS. Atmospheric pressure laser desorption/ionization of plant metabolites and plant tissue using colloidal graphite. Rapid Commun Mass Spectrom. 2010;24:397-402.
[100] Sroyraya M, Goto-Inoue N, Zaima N, Hayasaka T, Chansela P, Tanasawet S, et al. Visualization of biomolecules in the eyestalk of the blue swimming crab, portunus pelagicus, by imaging mass spectrometry using the atmospheric-pressure mass microscope. Surf Interface Anal. 2010;42:1589-92.
[101] Schober Y, Guenther S, Spengler B, Römpp A. Single cell matrix-assisted laser desorption/ionization mass spectrometry imaging. Anal Chem. 2012.
[102] Powell AK, Harvey DJ. Stabilization of sialic acids in n-linked oligosaccharides and gangliosides for analysis by positive ion matrix-assisted laser desorption/ionization mass spectrometry. Rapid Commun Mass Spectrom. 1996;10:1027-32.
[103] Ivleva VB, Elkin YN, Budnik BA, Moyer SC, O'Connor PB, Costello CE. Coupling thin-layer chromatography with vibrational cooling matrix-assisted laser desorption/ionization fourier transform mass spectrometry for the analysis of ganglioside mixtures. Anal Chem. 2004;76:6484-91.
[104] Berkenkamp S, Karas M, Hillenkamp F. Ice as a matrix for IR-matrix-assisted laser desorption/ionization: Mass spectra from a protein single crystal. Proc Nat Acad Sci. 1996;93:7003-7.
[105] Berkenkamp S, Menzel C, Karas M, Hillenkamp F. Performance of infrared matrix-assisted laser desorption/ionization mass spectrometry with lasers emitting in the 3 μm wavelength range. Rapid Commun Mass Spectrom. 1997;11:1399-406.
[106] Li Y, Shrestha B, Vertes A. Atmospheric pressure molecular imaging by infrared MALDI mass spectrometry. Anal Chem. 2007;79:523-32.
[107] Shrestha B, Nemes P, Nazarian J, Hathout Y, Hoffman EP, Vertes A. Direct analysis of lipids and small metabolites in mouse brain tissue by AP IR-MALDI and reactive LAESI mass spectrometry. Analyst. 2010;135:751-8.
[108] Dreisewerd K, Lemaire R, Pohlentz G, Salzet M, Wisztorski M, Berkenkamp S, et al. Molecular profiling of native and matrix-coated tissue slices from rat brain by infrared and ultraviolet laser desorption/ionization orthogonal time-of-flight mass spectrometry. Anal Chem. 2007;79:2463-71.
[109] Li Y, Shrestha B, Vertes A. Atmospheric pressure infrared MALDI imaging mass spectrometry for plant metabolomics. Anal Chem. 2008;80:407-20.

[110] Dreisewerd K, Draude F, Kruppe S, Rohlfing A, Berkenkamp S, Pohlentz G. Molecular analysis of native tissue and whole oils by infrared laser mass spectrometry. Anal Chem. 2007;79:4514-20.
[111] Dreisewerd K, Berkenkamp S, Leisner A, Rohlfing A, Menzel C. Fundamentals of matrix-assisted laser desorption/ionization mass spectrometry with pulsed infrared lasers. Int J Mass Spectrom. 2003;226:189-209.
[112] Dreisewerd K. The desorption process in MALDI. Chem Rev. 2003;103:395-426.
[113] Rohlfing A, Müthing J, Pohlentz G, Distler U, Peter-Katalinić J, Berkenkamp S, et al. IR-MALDI-MS analysis of HPTLC-separated phospholipid mixtures directly from the TLC plate. Anal Chem. 2007;79:5793-808.
[114] Dreisewerd K, Müthing J, Rohlfing A, Meisen I, Vukelić Ž, Peter-Katalinić J, et al. Analysis of gangliosides directly from thin-layer chromatography plates by infrared matrix-assisted laser desorption/ionization orthogonal ttime-of-flight mass spectrometry with a glycerol matrix. Anal Chem. 2005;77:4098-107.
[115] Souady J, Soltwisch J, Dreisewerd K, Haier Jr, Peter-Katalinić J, Müthing J. Structural profiling of individual glycosphingolipids in a single thin-layer chromatogram by multiple sequential immunodetection matched with direct IR-MALDI-o-TOF mass spectrometry. Anal Chem. 2009;81:9481-92.
[116] Park S-G, Murray KK. Infrared laser ablation sample transfer for MALDI imaging. Anal Chem. 2012;84:3240-5.
[117] Rousell DJ, Dutta SM, Little MW, Murray KK. Matrix-free infrared soft laser desorption/ionization. J Mass Spectrom. 2004;39:1182-9.
[118] Cramer R, Burlingame AL. Employing target modifications for the investigation of liquid infrared matrix-assisted laser desorption/ionization mass spectrometry. Rapid Commun Mass Spectrom. 2000;14:53-60.
[119] Sampson J, Hawkridge A, Muddiman D. Generation and detection of multiply-charged peptides and proteins by matrix-assisted laser desorption electrospray ionization (MALDESI) fourier transform ion cyclotron resonance mass spectrometry. J Am Soc Mass Spectrom. 2006;17:1712-6.
[120] Nemes P, Vertes A. Laser ablation electrospray ionization for atmospheric pressure, in vivo, and imaging mass spectrometry. Anal Chem. 2007;79:8098-106.
[121] Shiea J, Huang M-Z, Hsu H-J, Lee C-Y, Yuan C-H, Beech I, et al. Electrospray-assisted laser desorption/ionization mass spectrometry for direct ambient analysis of solids. Rapid Commun Mass Spectrom. 2005;19:3701-4.
[122] Park S-G, Murray K. Infrared laser ablation sample transfer for MALDI and electrospray. J Am Soc Mass Spectrom. 2011;22:1352-62.
[123] Nemes P, Woods AS, Vertes A. Simultaneous imaging of small metabolites and lipids in rat brain tissues at atmospheric pressure by laser ablation electrospray ionization mass spectrometry. Anal Chem. 2010;82:982-8.
[124] Huang M-Z, Jhang S-S, Cheng C-N, Cheng S-C, Shiea J. Effects of matrix, electrospray solution, and laser light on the desorption and ionization mechanisms in electrospray-assisted laser desorption ionization mass spectrometry. Analyst. 2010;135:759-66.
[125] Huang M-Z, Hsu H-J, Wu C-I, Lin S-Y, Ma Y-L, Cheng T-L, et al. Characterization of the chemical components on the surface of different solids with electrospray-assisted laser desorption ionization mass spectrometry. Rapid Commun Mass Spectrom. 2007;21:1767-75.
[126] Sripadi P, Shrestha B, Easley RL, Carpio L, Kehn-Hall K, Chevalier S, et al. Direct detection of diverse metabolic changes in virally transformed and tax-expressing cells by mass spectrometry. PLoS ONE. 2010;5:e12590.

[127] Shrestha B, Patt JM, Vertes A. In situ cell-by-cell imaging and analysis of small cell populations by mass spectrometry. Anal Chem. 2011;83:2947-55.
[128] Shrestha B, Vertes A. In situ metabolic profiling of single cells by laser ablation electrospray ionization mass spectrometry. Anal Chem. 2009;81:8265-71.
[129] Vaikkinen A, Shrestha B, Nazarian J, Kostiainen R, Vertes A, Kauppila TJ. Simultaneous detection of nonpolar and polar compounds by heat-assisted laser ablation electrospray ionization mass spectrometry. Anal Chem. 2012;85:177-84.
[130] Peterson DS. Matrix-free methods for laser desorption/ionization mass spectrometry. Mass Spectrom Rev. 2007;26:19-34.
[131] Wei J, Buriak JM, Siuzdak G. Desorption-ionization mass spectrometry on porous silicon. Nature. 1999;399:243-6.
[132] Go EP, Apon JV, Luo G, Saghatelian A, Daniels RH, Sahi V, et al. Desorption/ionization on silicon nanowires. Anal Chem. 2005;77:1641-6.
[133] Northen TR, Yanes O, Northen MT, Marrinucci D, Uritboonthai W, Apon J, et al. Clathrate nanostructures for mass spectrometry. Nature. 2007;449:1033-6.
[134] Cha S, Yeung ES. Colloidal graphite-assisted laser desorption/ionization mass spectrometry and MSn of small molecules. 1. Imaging of cerebrosides directly from rat brain tissue. Anal Chem. 2007;79:2373-85.
[135] Woo H-K, Northen TR, Yanes O, Siuzdak G. Nanostructure-initiator mass spectrometry: A protocol for preparing and applying NIMS surfaces for high-sensitivity mass analysis. Nat Protoc. 2008;3:1341-9.
[136] Muck A, Stelzner T, Hubner U, Christiansen S, Svatos A. Lithographically patterned silicon nanowire arrays for matrix free LDI-TOF/MS analysis of lipids. Lab on a Chip. 2010;10:320-5.
[137] Budimir N, Blais J-C, Fournier F, Tabet J-C. The use of desorption/ionization on porous silicon mass spectrometry for the detection of negative ions for fatty acids. Rapid Commun Mass Spectrom. 2006;20:680-4.
[138] Watanabe T, Kawasaki H, Yonezawa T, Arakawa R. Surface-assisted laser desorption/ionization mass spectrometry (SALDI-MS) of low molecular weight organic compounds and synthetic polymers using zinc oxide (ZnO) nanoparticles. J Mass Spectrom. 2008;43:1063-71.
[139] Daniels RH, Dikler S, Li E, Stacey C. Break free of the matrix: Sensitive and rapid analysis of small molecules using nanostructured surfaces and LDI-TOF mass spectrometry. JALA Charlottesv Va. 2008;13:314-21.
[140] Wyatt MF, Ding S, Stein BK, Brenton AG, Daniels RH. Analysis of various organic and organometallic compounds using nanostructure-assisted laser desorption/ionization time-of-flight mass spectrometry (NALDI-TOFMS). J Am Soc Mass Spectrom. 2010;21:1256-9.
[141] Kang M-J, Pyun J-C, Lee J-C, Choi Y-J, Park J-H, Park J-G, et al. Nanowire-assisted laser desorption and ionization mass spectrometry for quantitative analysis of small molecules. Rapid Commun Mass Spectrom. 2005;19:3166-70.
[142] Pavlaskova K, Strnadova M, Strohalm M, Havlicek V, Sulc M, Volny M. Time-dependent oxidation during nano-assisted laser desorption ionization mass spectrometry: A useful tool for structure determination or a source of possible confusion? Anal Chem. 2011;83:5661-5.
[143] Colantonio S, Simpson J, Fisher R, Yavlovich A, Belanger J, Puri A, et al. Quantitative analysis of phospholipids using nanostructured laser desorption ionization targets. Lipids. 2011;46:469-77.
[144] Guénin E, Lecouvey M, Hardouin J. Could a nano-assisted laser desorption/ionization target improve the study of small organic molecules by laser desorption/ionization time-of-flight mass spectrometry? Rapid Commun Mass Spectrom. 2009;23:1395-400.

. Laser desorption-ionization of lipid transfers: Tissue mass spectrometry imaging without MALDI matrix. Anal Chem. 2010;82:4994-7.
[146] Hsu PY, Ge LH, Li XP, Stark AY, Wesdemiotis C, Niewiarowski PH, et al. Direct evidence of phospholipids in gecko footprints and spatula-substrate contact interface detected using surface-sensitive spectroscopy. J R Soc Interface. 2012;9:657-64.
[147] Patti GJ, Shriver LP, Wassif CA, Woo HK, Uritboonthai W, Apon J, et al. Nanostructure-initiator mass spectrometry (NIMS) imaging of brain cholesterol metabolites in smith-lemli-opitz syndrome. Neuroscience. 2010;170:858-64.
[148] Lee DY, Platt V, Bowen B, Louie K, Canaria CA, McMurray CT, et al. Resolving brain regions using nanostructure initiator mass spectrometry imaging of phospholipids. Integr Biol. 2012.
[149] Yew JY, Dreisewerd K, Luftmann H, Müthing J, Pohlentz G, Kravitz EA. A new male sex pheromone and novel cuticular cues for chemical communication in drosophila. Curr Biol. 2009;19:1245-54.
[150] Yew J, Soltwisch J, Pirkl A, Dreisewerd K. Direct laser desorption ionization of endogenous and exogenous compounds from insect cuticles: Practical and methodologic aspects. J Am Soc Mass Spectrom. 2011;22:1273-84.
[151] Pachuta SJ, Cooks RG. Mechanisms in molecular SIMS. Chem Rev. 1987 87:647-69.
[152] Vickerman JC. Impact of mass spectrometry in surface analysis. Analyst. 1994;119:513-23.
[153] Galli Marxer C, Kraft ML, Weber PK, Hutcheon ID, Boxer SG. Supported membrane composition analysis by secondary ion mass spectrometry with high lateral resolution. Biophysical journal. 2005;88:2965-75.
[154] Fletcher JS, Rabbani S, Henderson A, Lockyer NP, Vickerman JC. Three-dimensional mass spectral imaging of HeLa-M cells – sample preparation, data interpretation and visualisation. Rapid Commun Mass Spectrom. 2011;25:925-32.
[155] Ostrowski SG, Van Bell CT, Winograd N, Ewing AG. Mass spectrometric imaging of highly curved membranes during tetrahymena mating. Science. 2004;305:71-3.
[156] Pacholski ML, Cannon DM, Ewing AG, Winograd N. Static time-of-flight secondary ion mass spectrometry imaging of freeze-fractured, frozen-hydrated biological membranes. Rapid Commun Mass Spectrom. 1998;12:1232-5.
[157] Colliver TL, Brummel CL, Pacholski ML, Swanek FD, Ewing AG, Winograd N. Atomic and molecular imaging at the single-cell level with TOF-SIMS. Anal Chem. 1997;69:2225-31.
[158] Fletcher J, Vickerman J. A new SIMS paradigm for 2D and 3D molecular imaging of bio-systems. Anal Bioanal Chem. 2010;396:85-104.
[159] Touboul D, Kollmer F, Niehuis E, Brunelle A, Laprévote O. Improvement of biological time-of-flight-secondary ion mass spectrometry imaging with a bismuth cluster ion source. J Am Soc Mass Spectrom. 2005;16:1608-18.
[160] Touboul D, Halgand F, Brunelle A, Kersting R, Tallarek E, Hagenhoff B, et al. Tissue molecular ion imaging by gold cluster ion bombardment. Anal Chem. 2004;76:1550-9.
[161] Weibel D, Wong S, Lockyer N, Blenkinsopp P, Hill R, Vickerman JC. A C_{60} primary ion beam system for time of flight secondary ion mass spectrometry: Its development and secondary ion yield characteristics. Anal Chem. 2003;75:1754-64.
[162] Ostrowski SG, Szakal C, Kozole J, Roddy TP, Xu J, Ewing AG, et al. Secondary ion MS imaging of lipids in picoliter vials with a buckminsterfullerene ion source. Anal Chem. 2005;77:6190-6.

[163] Jones EA, Lockyer NP, Vickerman JC. Mass spectral analysis and imaging of tissue by ToF-SIMS—the role of buckminsterfullerene, C_{60}^+, primary ions. Int J Mass Spectrom. 2007;260:146-57.
[164] Postawa Z, Czerwinski B, Szewczyk M, Smiley EJ, Winograd N, Garrison BJ. Enhancement of sputtering yields due to C_{60} versus ga bombardment of Ag{111} as explored by molecular dynamics simulations. Anal Chem. 2003;75:4402-7.
[165] Nygren H, Börner K, Hagenhoff B, Malmberg P, Månsson J-E. Localization of cholesterol, phosphocholine and galactosylceramide in rat cerebellar cortex with imaging TOF-SIMS equipped with a bismuth cluster ion source. Biochim Biophys Acta, Mol Cell Biol Lipids. 2005;1737:102-10.
[166] Wu KJ, Odom RW. Matrix-enhanced secondary ion mass spectrometry: A method for molecular analysis of solid surfaces. Anal Chem. 1996;68:873-82.
[167] McDonnell LA, Piersma SR, Altelaar AFM, Mize TH, Luxembourg SL, Verhaert PDEM, et al. Subcellular imaging mass spectrometry of brain tissue. J Mass Spectrom. 2005;40:160-8.
[168] Delcorte A. Matrix-enhanced secondary ion mass spectrometry: The alchemist's solution? Appl Surf Sci. 2006;252:6582-7.
[169] Luxembourg SL, McDonnell LA, Duursma MC, Guo X, Heeren RMA. Effect of local matrix crystal variations in matrix-assisted ionization techniques for mass spectrometry. Anal Chem. 2003;75:2333-41.
[170] Heeren RMA, McDonnell LA, Amstalden E, Luxembourg SL, Altelaar AFM, Piersma SR. Why don't biologists use SIMS?: A critical evaluation of imaging MS. Appl Surf Sci. 2006;252:6827-35.
[171] Fitzgerald JJD, Kunnath P, Walker AV. Matrix-enhanced secondary ion mass spectrometry (ME SIMS) using room temperature ionic liquid matrices. Anal Chem. 2010;82:4413-9.
[172] McDonnell LA, Heeren RMA, de Lange RPJ, Fletcher IW. Higher sensitivity secondary ion mass spectrometry of biological molecules for high resolution, chemically specific imaging. J Am Soc Mass Spectrom. 2006;17:1195-202.
[173] Nygren H, Malmberg P, Kriegeskotte C, Arlinghaus HF. Bioimaging TOF-SIMS: Localization of cholesterol in rat kidney sections. FEBS Lett. 2004;566:291-3.
[174] Altelaar AFM, Klinkert I, Jalink K, deLange RPJ, Adan RAH, Heeren RMA, et al. Gold-enhanced biomolecular surface imaging of cells and tissue by SIMS and MALDI mass spectrometry. Anal Chem. 2006;78:734-42.
[175] Carado A, Kozole J, Passarelli M, Winograd N, Loboda A, Bunch J, et al. Biological tissue imaging with a hybrid cluster SIMS quadrupole time-of-flight mass spectrometer. Appl Surf Sci. 2008;255:1572-5.
[176] Fletcher JS, Rabbani S, Henderson A, Blenkinsopp P, Thompson SP, Lockyer NP, et al. A new dynamic in mass spectral imaging of single biological cells. Anal Chem. 2008;80:9058-64.
[177] Smith DF, Robinson EW, Tolmachev AV, Heeren RMA, Paša-Tolić L. C_{60} secondary ion fourier transform ion cyclotron resonance mass spectrometry. Anal Chem. 2011;83:9552-6.
[178] Kertesz V, Berkel GJV. Improved imaging resolution in desorption electrospray ionization mass spectrometry. Rapid Commun Mass Spectrom. 2008;22:2639-44.
[179] Campbell D, Ferreira C, Eberlin L, Cooks R. Improved spatial resolution in the imaging of biological tissue using desorption electrospray ionization. Anal Bioanal Chem. 2012;404:389-98.
[180] Costa AB, Cooks RG. Simulation of atmospheric transport and droplet-thin film collisions in desorption electrospray ionisation. Chem Commun. 2007;38:3915.

[181] Costa AB, Graham Cooks R. Simulated splashes: Elucidating the mechanism of desorption electrospray ionization mass spectrometry. Chem Phys Lett. 2008;464:1-8.
[182] Manicke NE, Wiseman JM, Ifa DR, Cooks RG. Desorption electrospray ionization (DESI) mass spectrometry and tandem mass spectrometry (MS/MS) of phospholipids and sphingolipids: Ionization, adduct formation, and fragmentation. J Am Soc Mass Spectrom. 2008;19:531-43.
[183] Paglia G, Ifa DR, Wu C, Corso G, Cooks RG. Desorption electrospray ionization mass spectrometry analysis of lipids after two-dimensional high-performance thin-layer chromatography partial separation. Anal Chem. 2010;82:1744-50.
[184] Ellis SR, Hughes JR, Mitchell TW, in het Panhuis M, Blanksby SJ. Using ambient ozone for assignment of double bond position in unsaturated lipids. Analyst. 2012;137:1100-10.
[185] Ellis SR, Wu C, Deeley JM, Zhu X, Truscott RJW, in het Panhuis M, et al. Imaging of human lens lipids by desorption electrospray ionization mass spectrometry. J Am Soc Mass Spectrom. 2010;21:2095-104.
[186] Manicke NE, Dill AL, Ifa DR, Cooks RG. High-resolution tissue imaging on an orbitrap mass spectrometer by desorption electrospray ionization mass spectrometry. J Mass Spectrom. 2010;45:223-6.
[187] Wiseman JM, Puolitaiva SM, Takáts Z, Cooks RG, Caprioli RM. Mass spectrometric profiling of intact biological tissue by using desorption electrospray ionization. Angew Chem, Int Ed. 2005;44:7094-7.
[188] Girod M, Shi Y, Cheng J-X, Cooks R. Desorption electrospray ionization imaging mass spectrometry of lipids in rat spinal cord. J Am Soc Mass Spectrom. 2010;21:1177-89.
[189] Zhang JI, Talaty N, Costa AB, Xia Y, Tao WA, Bell R, et al. Rapid direct lipid profiling of bacteria using desorption electrospray ionization mass spectrometry. Int J Mass Spectrom. 2011;301:37-44.
[190] Basile F, Sibray T, Belisle JT, Bowen RA. Analysis of lipids from crude lung tissue extracts by desorption electrospray ionization mass spectrometry and pattern recognition. Anal Biochem. 2011;408:289-96.
[191] Eberlin LS, Norton I, Dill AL, Golby AJ, Ligon KL, Santagata S, et al. Classifying human brain tumors by lipid imaging with mass spectrometry. Cancer Res. 2012;72:645-54.
[192] Dill AL, Ifa DR, Manicke NE, Costa AB, Ramos-Vara JA, Knapp DW, et al. Lipid profiles of canine invasive transitional cell carcinoma of the urinary bladder and adjacent normal tissue by desorption electrospray ionization imaging mass spectrometry. Anal Chem. 2009;81:8758-64.
[193] Eberlin LS, Dill AL, Golby AJ, Ligon KL, Wiseman JM, Cooks RG, et al. Discrimination of human astrocytoma subtypes by lipid analysis using desorption electrospray ionization imaging mass spectrometry. Angew Chem, Int Ed. 2010;49:5953-6.
[194] Wiseman JM, Li JB. Elution, partial separation, and identification of lipids directly from tissue slices on planar chromatography media by desorption electrospray ionization mass spectrometry. Anal Chem. 2010;82:8866-74.
[195] Gerbig S, Takáts Z. Analysis of triglycerides in food items by desorption electrospray ionization mass spectrometry. Rapid Commun Mass Spectrom. 2010;24:2186-92.
[196] Gerbig S, Golf O, Balog J, Denes J, Baranyai Z, Zarand A, et al. Analysis of colorectal adenocarcinoma tissue by desorption electrospray ionization mass spectrometric imaging. Anal Bioanal Chem. 2012;403:2315-25.
[197] Jackson AU, Shum T, Sokol E, Dill A, Cooks RG. Enhanced detection of olefins using ambient ionization mass spectrometry: Ag adducts of biologically relevant alkenes. Anal Bioanal Chem. 2011;399:367-76.

[198] Girod M, Shi Y, Cheng J-X, Cooks RG. Mapping lipid alterations in traumatically injured rat spinal cord by desorption electrospray ionization imaging mass spectrometry. Anal Chem. 2010;83:207-15.
[199] Wu C, Ifa DR, Manicke NE, Cooks RG. Rapid, direct analysis of cholesterol by charge labeling in reactive desorption electrospray ionization. Anal Chem. 2009;81:7618-24.
[200] Wu C, Ifa DR, Manicke NE, Cooks RG. Molecular imaging of adrenal gland by desorption electrospray ionization mass spectrometry. Analyst. 2010;135:28-32.
[201] Manicke NE, Nefliu M, Wu C, Woods JW, Reiser V, Hendrickson RC, et al. Imaging of lipids in atheroma by desorption electrospray ionization mass spectrometry. Anal Chem. 2009;81:8702-7.
[202] Suni NM, Aalto H, Kauppila TJ, Kotiaho T, Kostiainen R. Analysis of lipids with desorption atmospheric pressure photoionization-mass spectrometry (DAPPI-MS) and desorption electrospray ionization-mass spectrometry (DESI-MS). J Mass Spectrom. 2012;47:611-9.
[203] Nyadong L, Late S, Green MD, Banga A, Fernández FM. Direct quantitation of active ingredients in solid artesunate antimalarials by noncovalent complex forming reactive desorption electrospray ionization mass spectrometry. J Am Soc Mass Spectrom. 2008;19:380-8.
[204] Song Y, Cooks RG. Reactive desorption electrospray ionization for selective detection of the hydrolysis products of phosphonate esters. J Mass Spectrom. 2007;42:1086-92.
[205] Zhang Y, Chen H. Detection of saccharides by reactive desorption electrospray ionization (DESI) using modified phenylboronic acids. Int J Mass Spectrom. 2010;289:98-107.
[206] Chen H, Cotte-Rodriguez I, Cooks RG. cis-diol functional group recognition by reactive desorption electrospray ionization (DESI). Chem Commun. 2006:597-9.
[207] Girod M, Moyano E, Campbell DI, Cooks RG. Accelerated bimolecular reactions in microdroplets studied by desorption electrospray ionization mass spectrometry. Chem Sci. 2011;2:501-10.
[208] Wu C, Qian K, Nefliu M, Cooks RG. Ambient analysis of saturated hydrocarbons using discharge-induced oxidation in desorption electrospray ionization. J Am Soc Mass Spectrom. 2010;21:261-7.
[209] Jackson AU, Werner SR, Talaty N, Song Y, Campbell K, Cooks RG, et al. Targeted metabolomic analysis of escherichia coli by desorption electrospray ionization and extractive electrospray ionization mass spectrometry. Anal Biochem. 2008;375:272-81.
[210] Ferreira CR, Eberlin LS, Hallett JE, Cooks RG. Single ocyte and single embryo lipid analysis by desorption electrospray ionization mass spectrometry. J Mass Spectrom. 2012;47:29-33.
[211] Dill A, Eberlin L, Zheng C, Costa A, Ifa D, Cheng L, et al. Multivariate statistical differentiation of renal cell carcinomas based on lipidomic analysis by ambient ionization imaging mass spectrometry. Anal Bioanal Chem. 2010;398:2969-78.
[212] Masterson T, Dill A, Eberlin L, Mattarozzi M, Cheng L, Beck S, et al. Distinctive glycerophospholipid profiles of human seminoma and adjacent normal tissues by desorption electrospray ionization imaging mass spectrometry. J Am Soc Mass Spectrom. 2011;22:1326-33.
[213] Eberlin LS, Dill AL, Costa AB, Ifa DR, Cheng L, Masterson T, et al. Cholesterol sulfate imaging in human prostate cancer tissue by desorption electrospray ionization mass spectrometry. Anal Chem. 2010;82:3430-4.
[214] Eberlin LS, Ferreira CR, Dill AL, Ifa DR, Cheng L, Cooks RG. Nondestructive, histologically compatible tissue imaging by desorption electrospray ionization mass spectrometry. ChemBioChem. 2011;12:2129-32.

[215] Eberlin LS, Liu X, Ferreira CR, Santagata S, Agar NYR, Cooks RG. Desorption electrospray ionization then MALDI mass spectrometry imaging of lipid and protein distributions in single tissue sections. Anal Chem. 2011;83:8366-71.
[216] Hirabayashi A, Sakairi M, Koizumi H. Sonic spray ionization method for atmospheric pressure ionization mass spectrometry. Anal Chem. 1994;66:4557-9.
[217] Cardoso K, Da Silva M, Grimaldi R, Stahl M, Simas R, Cunha I, et al. TAG profiles of *jatropha curcas* l. Seed oil by easy ambient sonic-spray ionization mass spectrometry. J Am Oil Chem Soc. 2012;89:67-71.
[218] Riccio MF, Saraiva SA, Marques LA, Alberici R, Haddad R, Moller JC, et al. Easy mass spectrometry for metabolomics and quality control of vegetable and animal fats. Eur J Lipid Sci Technol. 2010;112:434-8.
[219] Simas RC, Catharino RR, Cunha IBS, Cabral EC, Barrera-Arellano D, Eberlin MN, et al. Instantaneous characterization of vegetable oils via TAG and FFA profiles by easy ambient sonic-spray ionization mass spectrometry. Analyst. 2010;135:738-44.
[220] Alberici L, Oliveira H, Catharino R, Vercesi A, Eberlin M, Alberici R. Distinct hepatic lipid profile of hypertriglyceridemic mice determined by easy ambient sonic-spray ionization mass spectrometry. Anal Bioanal Chem. 2011;401:1655-63.
[221] Janfelt C, Nørgaard A. Ambient mass spectrometry imaging: A comparison of desorption ionization by sonic spray and electrospray. J Am Soc Mass Spectrom. 2012:1-9.
[222] Schäfer K-C, Balog J, Szaniszló T, Szalay D, Mezey G, Dénes J, et al. Real time analysis of brain tissue by direct combination of ultrasonic surgical aspiration and sonic spray mass spectrometry. Anal Chem. 2011;83:7729-35.
[223] Schäfer K-C, Dénes J, Albrecht K, Szaniszló T, Balog J, Skoumal R, et al. In vivo, in situ tissue analysis using rapid evaporative ionization mass spectrometry. Angew Chem, Int Ed. 2009;48:8240-2.
[224] Luftmann H. A simple device for the extraction of TLC spots: Direct coupling with an electrospray mass spectrometer. Anal Bioanal Chem. 2004;378:964-8.
[225] Van Berkel GJ, Kertesz V. Application of a liquid extraction based sealing surface sampling probe for mass spectrometric analysis of dried blood spots and mouse whole-body thin tissue sections. Anal Chem. 2009;81:9146-52.
[226] Alpmann A, Morlock G. Improved online coupling of planar chromatography with electrospray mass spectrometry: Extraction of zones from glass plates. Anal Bioanal Chem. 2006;386:1543-51.
[227] Kertesz V, Van Berkel GJ. Fully automated liquid extraction-based surface sampling and ionization using a chip-based robotic nanoelectrospray platform. J Mass Spectrom. 2010;45:252-60.
[228] Van Berkel GJ, Sanchez AD, Quirke JME. Thin-layer chromatography and electrospray mass spectrometry coupled using a surface sampling probe. Anal Chem. 2002;74:6216-23.
[229] Wachs T, Henion J. Electrospray device for coupling microscale separations and other miniaturized devices with electrospray mass spectrometry. Anal Chem. 2001;73:632-8.
[230] Stegemann C, Drozdov I, Shalhoub J, Humphries J, Ladroue C, Didangelos A, et al. Comparative lipidomics profiling of human atherosclerotic plaques / clinical perspective. Circ Cardiovasc Genet. 2011;4:232-42.
[231] Brown SHJ, Huxtable LH, Willcox MDP, Blanksby SJ, Mitchell TW. Automated surface sampling of lipids from worn contact lenses coupled with tandem mass spectrometry. Analyst. 2013.
[232] Ellis SR, Ferris CJ, Gilmore KJ, Mitchell TW, Blanksby SJ, in het Panhuis M. Direct lipid profiling of single cells from inkjet printed microarrays. Anal Chem. 2012;84:9679-83.

[233] Berzina Z, Almeida R, Husen P, Vogt J, Baumgart J, Nitsch R, et al. Profiling spatial lipid species distribution in mouse brain by liquid extraction surface analysis. 60th ASMS Conference on Mass Spectrometry and Allied Topics. Vancouver, Canada2012.
[234] Laskin J, Heath BS, Roach PJ, Cazares L, Semmes OJ. Tissue imaging using nanospray desorption electrospray ionization mass spectrometry. Anal Chem. 2011;84:141-8.
[235] Watrous J, Roach P, Alexandrov T, Heath BS, Yang JY, Kersten RD, et al. Mass spectral molecular networking of living microbial colonies. Proc Nat Acad Sci. 2012;109:E1743–E52.
[236] Walworth MJ, Stankovich JJ, Van Berkel GJ, Schulz M, Minarik S, Nichols J, et al. Hydrophobic treatment enabling analysis of wettable surfaces using a liquid microjunction surface sampling probe/electrospray ionization-mass spectrometry system. Anal Chem. 2011;83:591-7.
[237] Byrdwell W. Atmospheric pressure chemical ionization mass spectrometry for analysis of lipids. Lipids. 2001;36:327-46.
[238] McEwen CN, McKay RG, Larsen BS. Analysis of solids, liquids, and biological tissues using solids probe introduction at atmospheric pressure on commercial LC/MS instruments. Anal Chem. 2005;77:7826-31.
[239] McEwen C, Gutteridge S. Analysis of the inhibition of the ergosterol pathway in fungi using the atmospheric solids analysis probe (ASAP) method. J Am Soc Mass Spectrom. 2007;18:1274-8.
[240] Galhena AS, Harris GA, Nyadong L, Murray KK, Fernandez FM. Small molecule ambient mass spectrometry imaging by infrared laser ablation metastable-induced chemical ionization. Anal Chem. 2010;82:2178-81.
[241] Vaclavik L, Cajka T, Hrbek V, Hajslova J. Ambient mass spectrometry employing direct analysis in real time (DART) ion source for olive oil quality and authenticity assessment. Anal Chim Acta. 2009;645:56-63.
[242] Pierce CY, Barr JR, Cody RB, Massung RF, Woolfitt AR, Moura H, et al. Ambient generation of fatty acid methyl ester ions from bacterial whole cells by direct analysis in real time (DART) mass spectrometry. Chem Commun. 2007:807-9.
[243] Yew JY, Cody RB, Kravitz EA. Cuticular hydrocarbon analysis of an awake behaving fly using direct analysis in real-time time-of-flight mass spectrometry. Proc Nat Acad Sci. 2008;105:7135-40.
[244] Cody RB. Observation of molecular ions and analysis of nonpolar compounds with the direct analysis in real time ion source. Anal Chem. 2009;81:1101-7.
[245] Harris G, Hostetler D, Hampton C, Fernández F. Comparison of the internal energy deposition of direct analysis in real time and electrospray ionization time-of-flight mass spectrometry. J Am Soc Mass Spectrom. 2010;21:855-63.
[246] Curtis M, Minier M, Chitranshi P, Sparkman O, Jones P, Xue L. Direct analysis in real time (DART) mass spectrometry of nucleotides and nucleosides: Elucidation of a novel fragment $[C_5H_5]^+$ and its in-source adducts. J Am Soc Mass Spectrom. 2010;21:1371-81.
[247] Morlock G, Ueda Y. New coupling of planar chromatography with direct analysis in real time mass spectrometry. J Chromatogr A. 2007;1143:243-51.
[248] Harper JD, Charipar NA, Mulligan CC, Zhang X, Cooks RG, Ouyang Z. Low-temperature plasma probe for ambient desorption ionization. Anal Chem. 2008;80:9097-104.
[249] Chan GCY, Shelley JT, Wiley JS, Engelhard C, Jackson AU, Cooks RG, et al. Elucidation of reaction mechanisms responsible for afterglow and reagent-ion formation in the low-temperature plasma probe ambient ionization source. Anal Chem. 2011;83:3675-86.
[250] Zhang JI, Tao WA, Cooks RG. Facile determination of double bond position in unsaturated fatty acids and esters by low temperature plasma ionization mass spectrometry. Anal Chem. 2011;83:4738-44.

[251] García-Reyes JF, Mazzoti F, Harper JD, Charipar NA, Oradu S, Ouyang Z, et al. Direct olive oil analysis by low-temperature plasma (LTP) ambient ionization mass spectrometry. Rapid Commun Mass Spectrom. 2009;23:3057-62.
[252] Zhang JI, Costa AB, Tao WA, Cooks RG. Direct detection of fatty acid ethyl esters using low temperature plasma (LTP) ambient ionization mass spectrometry for rapid bacterial differentiation. Analyst. 2011;136:3091-7.
[253] Haapala M, Pol J, Saarela V, Arvola V, Kotiaho T, Ketola RA, et al. Desorption atmospheric pressure photoionization. Anal Chem. 2007;79:7867-72.
, Saarela V, Franssila S, et al. Desorption and ionization mechanisms in desorption atmospheric pressure photoionization. Anal Chem. 2008;80:7460-6.
[255] Raffaelli A, Saba A. Atmospheric pressure photoionization mass spectrometry. Mass Spectrom Rev. 2003;22:318-31.
P, Lemr K, et al. Automated ambient desorption−ionization platform for surface imaging integrated with a commercial fourier transform ion cyclotron resonance mass spectrometer. Anal Chem. 2009;81:8479-87.
[257] Vaikkinen A, Shrestha B, Kauppila TJ, Vertes A, Kostiainen R. Infrared laser ablation atmospheric pressure photoionization mass spectrometry. Anal Chem. 2012;84:1630-6.
[258] Hiraoka K, Nishidate K, Mori K, Asakawa D, Suzuki S. Development of probe electrospray using a solid needle. Rapid Commun Mass Spectrom. 2007;21:3139-44.
[259] Yoshimura K, Chen LC, Yu Z, Hiraoka K, Takeda S. Real-time analysis of living animals by electrospray ionization mass spectrometry. Anal Biochem. 2011;417:195-201.
[260] Chen LC, Nishidate K, Saito Y, Mori K, Asakawa D, Takeda S, et al. Application of probe electrospray to direct ambient analysis of biological samples. Rapid Commun Mass Spectrom. 2008;22:2366-74.
[261] Chen LC, Yoshimura K, Yu Z, Iwata R, Ito H, Suzuki H, et al. Ambient imaging mass spectrometry by electrospray ionization using solid needle as sampling probe. J Mass Spectrom. 2009;44:1469-77.
[262] Chen LC, Nishidate K, Saito Y, Mori K, Asakawa D, Takeda S, et al. Characteristics of probe electrospray generated from a solid needle. The Journal of Physical Chemistry B. 2008;112:11164-70.
[263] Masujima T. Live single-cell mass spectrometry. Analytical Sciences. 2009;25:953-60.
[264] Liu J, Wang H, Manicke NE, Lin J-M, Cooks RG, Ouyang Z. Development, characterization, and application of paper spray ionization. Anal Chem. 2010;82:2463-71.
[265] Wang H, Liu J, Cooks RG, Ouyang Z. Paper spray for direct analysis of complex mixtures using mass spectrometry. Angew Chem, Int Ed. 2010;49:877-80.
[266] Li A, Wang H, Ouyang Z, Cooks RG. Paper spray ionization of polar analytes using non-polar solvents. Chem Commun. 2011;47:2811-3.
[267] Zhang Z, Xu W, Manicke NE, Cooks RG, Ouyang Z. Silica coated paper substrate for paper-spray analysis of therapeutic drugs in dried blood spots. Anal Chem. 2011;84:931-8.
[268] Wang H, Manicke NE, Yang Q, Zheng L, Shi R, Cooks RG, et al. Direct analysis of biological tissue by paper spray mass spectrometry. Anal Chem. 2011;83:1197-201.
[269] Cheng S-C, Huang M-Z, Shiea J. Thin-layer chromatography/laser-induced acoustic desorption/electrospray ionization mass spectrometry. Anal Chem. 2009;81:9274-81.
[270] Campbell JL, Crawford KE, Kenttämaa HI. Analysis of saturated hydrocarbons by using chemical ionization combined with laser-induced acoustic desorption/fourier transform ion cyclotron resonance mass spectrometry. Anal Chem. 2004;76:959-63.
[271] Cheng S-C, Cheng T-L, Chang H-C, Shiea J. Using laser-induced acoustic desorption/electrospray ionization mass spectrometry to characterize small organic and large

biological compounds in the solid state and in solution under ambient conditions. Anal Chem. 2008;81:868-74.
[272] Gao J, Borton D, Owen B, Jin Z, Hurt M, Amundson L, et al. Laser-induced acoustic desorption/atmospheric pressure chemical ionization mass spectrometry. J Am Soc Mass Spectrom. 2011;22:531-8.
[273] Jin Z, Daiya S, Kenttämaa HI. Characterization of nonpolar lipids and selected steroids by using laser-induced acoustic desorption/chemical ionization, atmospheric pressure chemical ionization, and electrospray ionization mass spectrometry. Int J Mass Spectrom. 2011;301:234-9.
[274] Landgraf RR, Garrett TJ, Prieto Conaway MC, Calcutt NA, Stacpoole PW, Yost RA. Considerations for quantification of lipids in nerve tissue using matrix-assisted laser desorption/ionization mass spectrometric imaging. Rapid Commun Mass Spectrom. 2011;25:3178-84.
[275] Manicke NE, Yang Q, Wang H, Oradu S, Ouyang Z, Cooks RG. Assessment of paper spray ionization for quantitation of pharmaceuticals in blood spots. Int J Mass Spectrom. 2011;300:123-9.
[276] Lanekoff I, Thomas M, Carson JP, Smith JN, Timchalk C, Laskin J. Imaging nicotine in rat brain tissue by use of nanospray desorption electrospray ionization mass spectrometry. Anal Chem. 2012;85:882-9.

Figure Captions

Fig 1. Schematic representations of (a) matrix-assisted laser desorption ionization (MALDI); (b) laser ablation electrospray ionization (LAESI); and (c) nanowire-assisted laser desorption ionization (NALDI) and nanostructure-initiator mass spectrometry (NIMS). UV-lasers are typically nitrogen (337 nm) or Nd:YAG (355 nm) lasers. IR-lasers are typically Er:YAG or OPO emitting at 2.94 μm.

Fig 2. Comparison of conventional (a) α-cyano-4-hydroxycinnamic acid (CHCA) and (b) 2,5-dihydroxybenzoic acid (DHB) matrices with (c) 1,8-bis(dimethylamino)naphthalene (DMAN) for negative ion fatty acid detection. Matrices were mixed 1:1 with stearic acid (18:0) and deposited onto a metallic target. The expected $[M-H]^-$ ion of stearic acid at *m/z* 283 (spectral region highlighted in red) is virtually absent and accompanied by significant matrix-related peaks when using CHCA and DHB. Analysis with DMAN reveals the $[M-H]^-$ ion in the absence of any matrix-related background. Adapted with permission from reference [66].

Fig 3. Thin-layer chromatography plate stained with primuline following separation of human brain lipid extract. Brain regions investigated were gray matter of the inferior frontal gyrus (lane 1), gray matter of the hippocampus (lane 2), white matter of the inferior frontal gyrus (lane 3), and white matter of the hippocampus (lane 4). Lipids were then transferred to a polyvinylidene difluoride (PVDF) membrane and analyzed by MALDI using 2,5-dihydroxybenzoic acid as the matrix. (b) MALDI spectrum acquired from region of the TLC plate containing phosphatidylcholine (PC) lipids and (c) sphingomyelin (SM) lipids. Adapted with permission from reference [34].

Fig. 4. Comparison of (a) Au^+ and (b) C_{60}^+ ion beams for phospholipid detection from a rat brain tissue section. Intact phospholipids are observed from *m/z* 700-800. Image adapted with permission from reference [163].

Fig. 5. Schematic representations of (a) desorption electrospray ionization (DESI) and (b) liquid extraction surface analysis (LESA).

Fig. 6. Reactive DESI mass spectra obtained using betaine aldehyde (BA) doped into the spray solution acquired from (a) a rat brain section where intact cholesterol is observed at *m/z* 488 and (b) a vacuum gas oil distillate deposited on glass. Saturated hydrocarbons are detected following *in situ* discharge-induced oxidation and reaction with BA. Images adapted with permission from references [199, 208].

Fig. 7. (a) Collision-induced dissociation (CID) spectrum of $[SM\ (d18:0/24:1)+Na]^+$ acquired from a human lens extract on a TLC plate. (b) DESI-MS spectra acquired from the region of a TLC containing sphingomyelins (SM) following separation of a human lens lipid extract. The most abundant unsaturated SM, $[SM\ (d18:0/24:1)+Na]^+$, is labeled with "*". Ozonolysis products arising from $[SM\ (d18:0/24:1)+Na]^+$ are also labeled. ■ = ozonolysis products originating from the *n*-9 isomer. ♦ = ozonolysis products originating from the *n*-7 isomer. ● = ozonolysis products originating from the *n*-5 isomer. Figure (b) adapted with permission from reference [184].

Fig. 8. (a) Coupling ultrasonic surgery handpiece to a mass spectrometer using a V-EASI source. Tissue debris is carried up the handpiece to the V-EASI source. (b) Positive ion spectrum of a porcine brain cortex following tissue ablation using the ultrasonic surgery handpiece and analysis by V-EASI-MS. Adapted with permission from reference [222].

Fig. 9. Liquid extraction surface analysis (LESA) mass spectra obtained from a (a) single L929 cell and (b) single PC12 cell. Both spectra were obtained using a precursor ion scan in positive ion mode for the phosphocholine headgroup (*m/z* 184.1) and thus reveal the phosphatidylcholine (PC) and sphingomyelin (SM) composition of each cell. Several abundant lipid ions are labeled. Image modified with permission from reference [232] .

Fig. 10. Schematic representations of (a) atmospheric pressure solids analysis probe (ASAP), and (b) the low temperature plasma (LTP) probe.

Fig. 11. Positive ion low temperature plasma mass spectrometry (LTP-MS) analysis of two 18:1 fatty acid methyl ester isomers with ozone produced by the dielectric barrier discharge. (a) *cis*-7-octadecanoic methyl ester (*n*-11) and (b) *cis*-12-octadecanoic acid methyl ester (*n*-6). Image adapted with permission from reference [250].

Fig 12. Schematic representations of (a) probe electrospray ionization (PESI) and (b) paper spray ionization.

Figures

Fig 1.

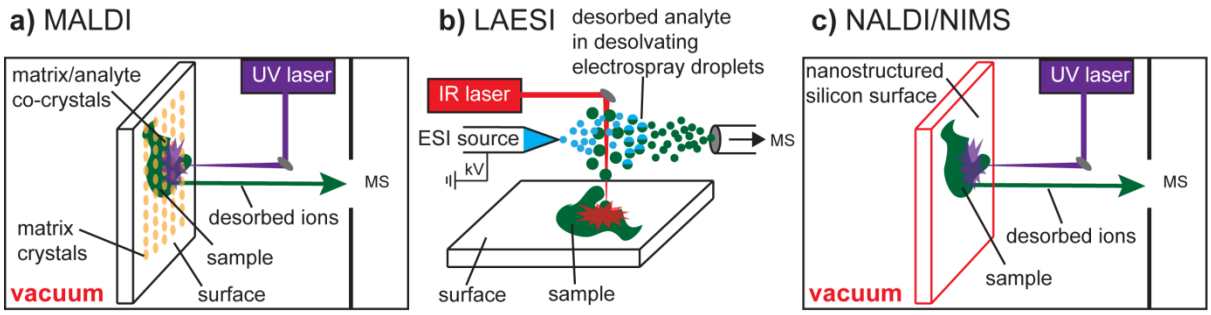

Fig 2.

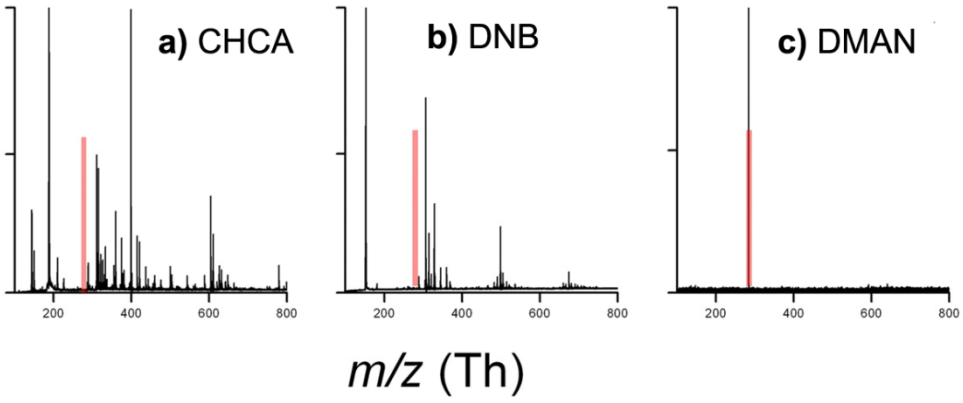

Fig 3.

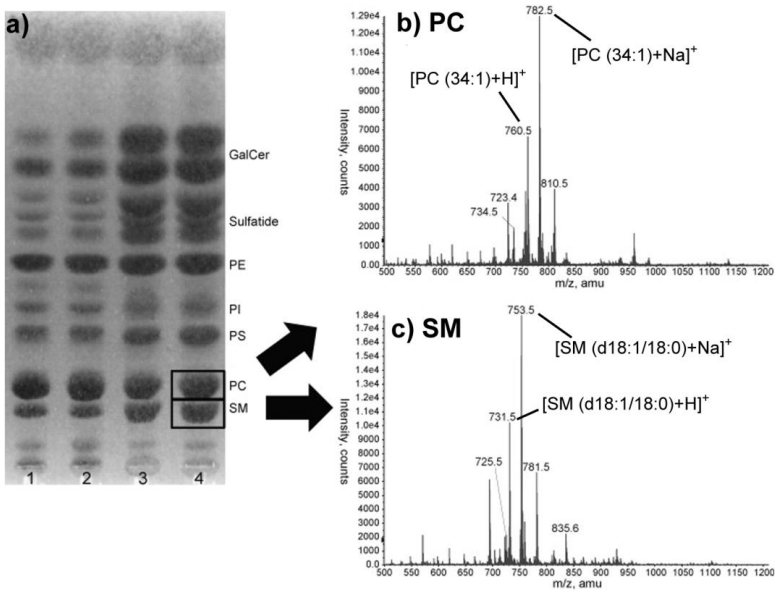
a)
GalCer
Sulfatide
PE
PI
PS
PC
SM
1
2
3
4
b) PC
[PC (34:1)+Na]+
[PC (34:1)+H]+
782.5
760.5
723.4
734.5
810.5
Intensity, counts
m/z, amu
c) SM
[SM (d18:1/18:0)+Na]+
[SM (d18:1/18:0)+H]+
753.5
731.5
725.5
781.5
835.6
Intensity, counts
m/z, amu

Fig. 4.

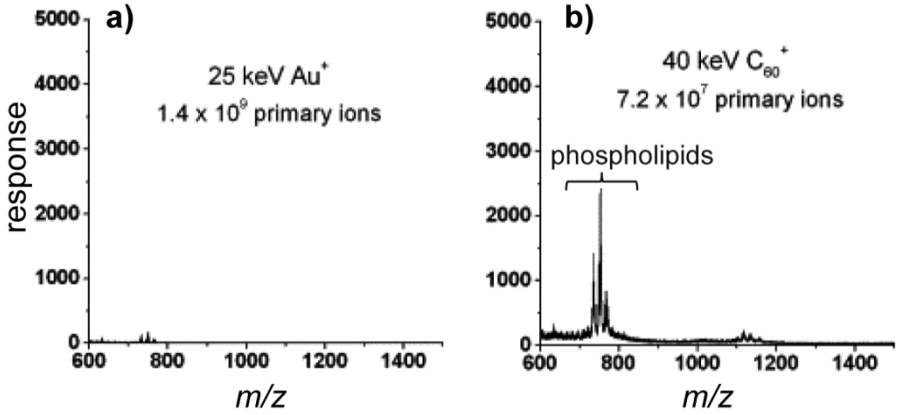
a)
25 keV Au+
1.4 x 10^9 primary ions
response
m/z
b)
40 keV C60+
7.2 x 10^7 primary ions
phospholipids
m/z

Fig. 5.

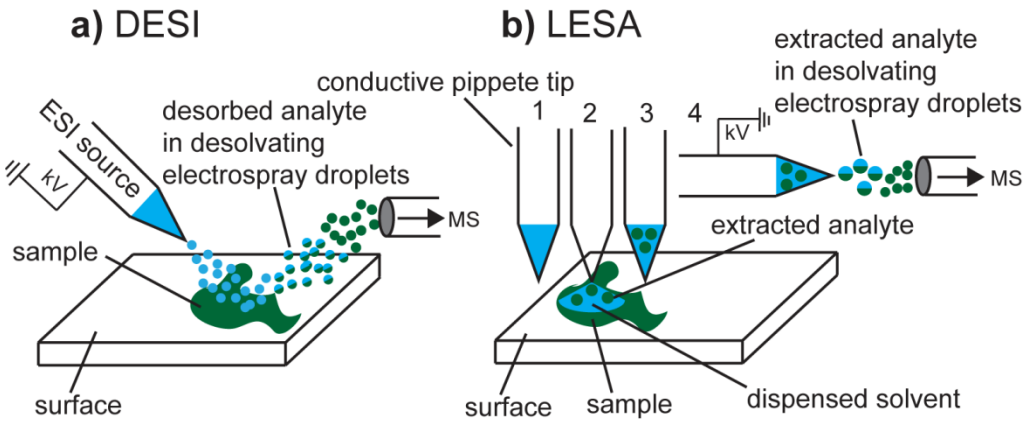
a) DESI
b) LESA
ESI source
kV
desorbed analyte
in desolvating
electrospray droplets
MS
sample
surface
conductive pippete tip
1
2
3
4
kV
extracted analyte
in desolvating
electrospray droplets
MS
extracted analyte
surface
sample
dispensed solvent

Fig. 6.

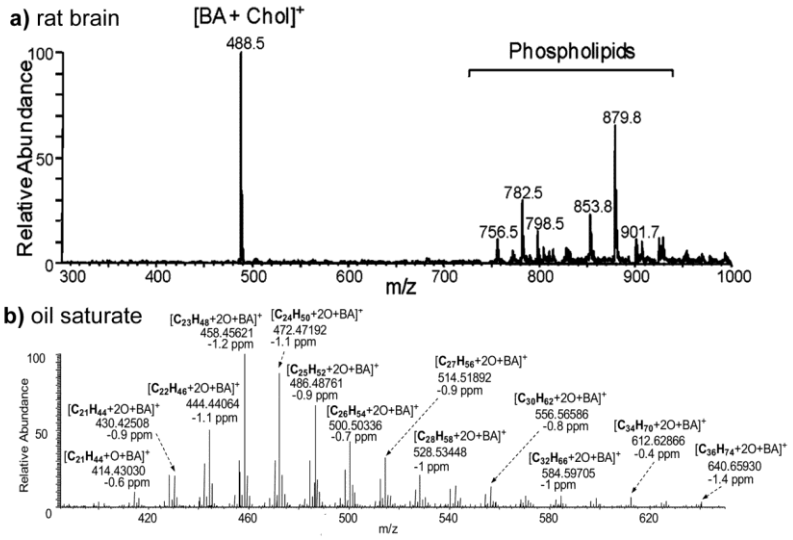
a) rat brain
[BA + Chol]+
488.5
Phospholipids
879.8
782.5
853.8
798.5
756.5
901.7
Relative Abundance
m/z
b) oil saturate
[C23H48+2O+BA]+ 458.45621 -1.2 ppm
[C24H50+2O+BA]+ 472.47192 -1.1 ppm
[C25H52+2O+BA]+ 486.48761 -0.9 ppm
[C27H56+2O+BA]+ 514.51892 -0.9 ppm
[C22H46+2O+BA]+ 444.44064 -1.1 ppm
[C21H44+2O+BA]+ 430.42508 -0.9 ppm
[C26H54+2O+BA]+ 500.50336 -0.7 ppm
[C30H62+2O+BA]+ 556.56586 -0.8 ppm
[C28H58+2O+BA]+ 528.53448 -1 ppm
[C34H70+2O+BA]+ 612.62866 -0.4 ppm
[C36H74+2O+BA]+ 640.65930 -1.4 ppm
[C32H66+2O+BA]+ 584.59705 -1 ppm
[C21H44+O+BA]+ 414.43030 -0.6 ppm
Relative Abundance
m/z

Fig. 7.

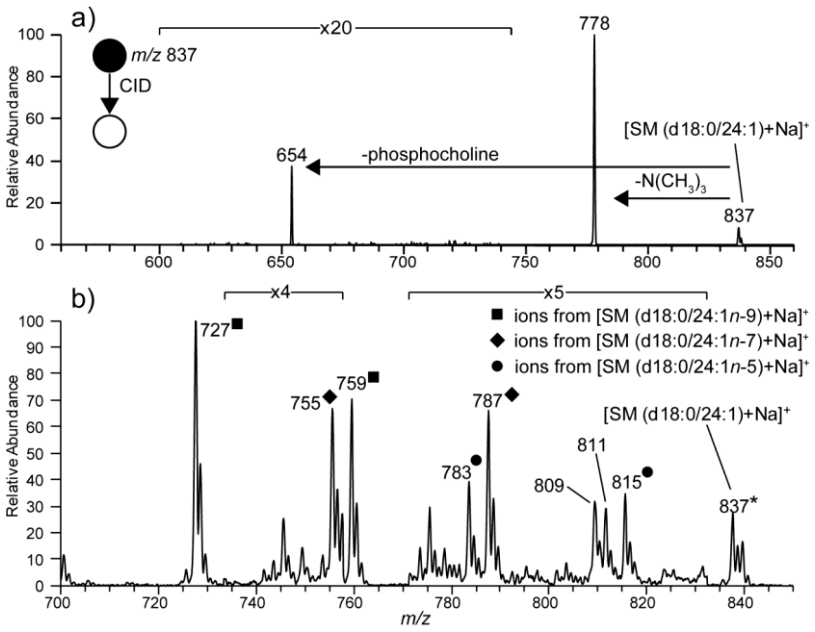
a)
x20
778
m/z 837
CID
[SM (d18:0/24:1)+Na]+
654
-phosphocholine
-N(CH3)3
837
Relative Abundance
b)
x4
x5
ions from [SM (d18:0/24:1n-9)+Na]+
ions from [SM (d18:0/24:1n-7)+Na]+
ions from [SM (d18:0/24:1n-5)+Na]+
727
759
755
787
[SM (d18:0/24:1)+Na]+
811
783
809
815
837*
Relative Abundance
m/z

Fig. 8.

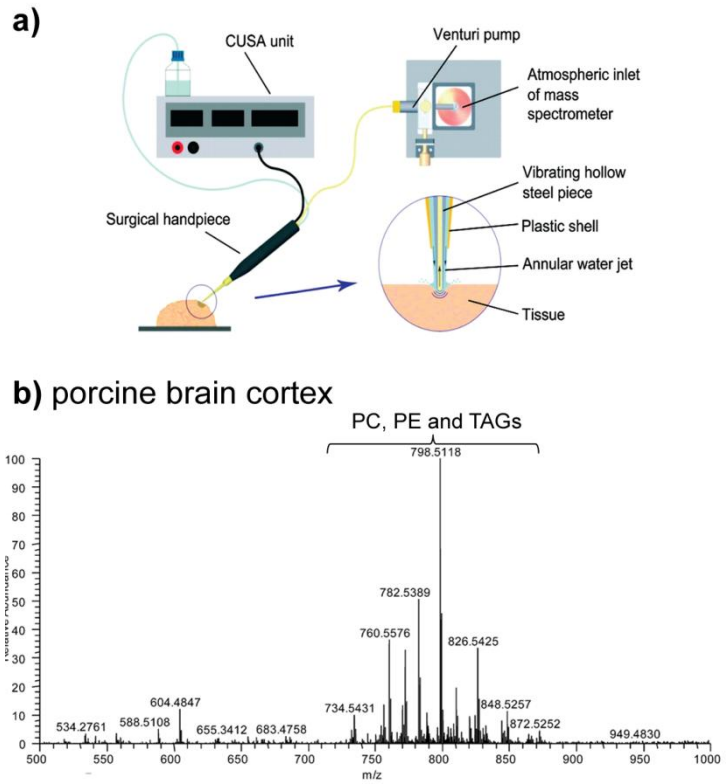
a)
CUSA unit
Venturi pump
Atmospheric inlet of mass spectrometer
Vibrating hollow steel piece
Plastic shell
Annular water jet
Surgical handpiece
Tissue
b) porcine brain cortex
PC, PE and TAGs
798.5118
782.5389
760.5576
826.5425
604.4847
588.5108
534.2761
655.3412
683.4758
734.5431
848.5257
872.5252
949.4830
m/z

Fig. 9.

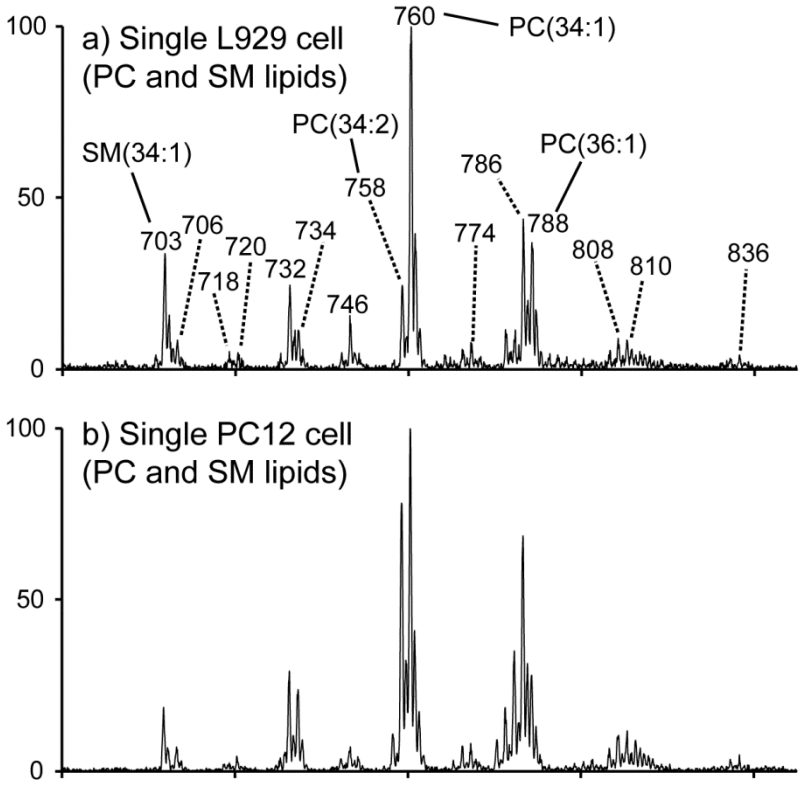
100
a) Single L929 cell
(PC and SM lipids)
760
PC(34:1)
PC(34:2)
758
SM(34:1)
703
706
718
720
732
734
746
786
774
PC(36:1)
788
808
810
836
50
0
100
b) Single PC12 cell
(PC and SM lipids)
50
0

Fig. 10.

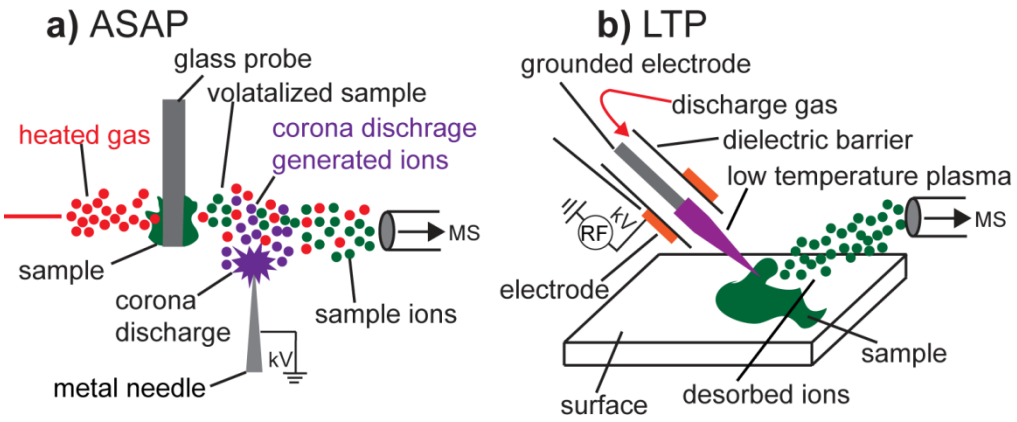
a) ASAP
glass probe
volatalized sample
heated gas
corona dischrage
generated ions
MS
sample
corona
discharge
sample ions
kV
metal needle
b) LTP
grounded electrode
discharge gas
dielectric barrier
low temperature plasma
RF
kV
MS
electrode
sample
surface
desorbed ions

Fig. 11.

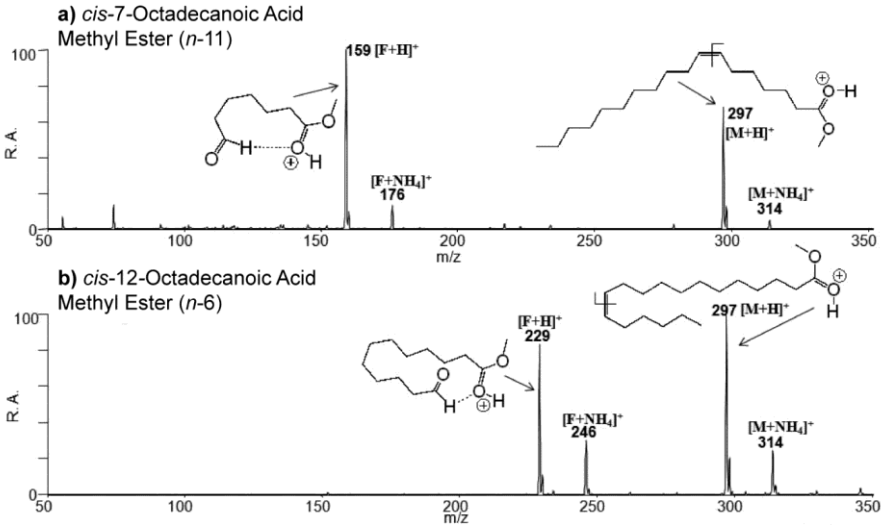
a) cis-7-Octadecanoic Acid
Methyl Ester (n-11)
159 [F+H]+
297
[M+H]+
[F+NH4]+
176
[M+NH4]+
314
R.A.
m/z
b) cis-12-Octadecanoic Acid
Methyl Ester (n-6)
297 [M+H]+
[F+H]+
229
[F+NH4]+
246
[M+NH4]+
314
R.A.
m/z

Fig 12.

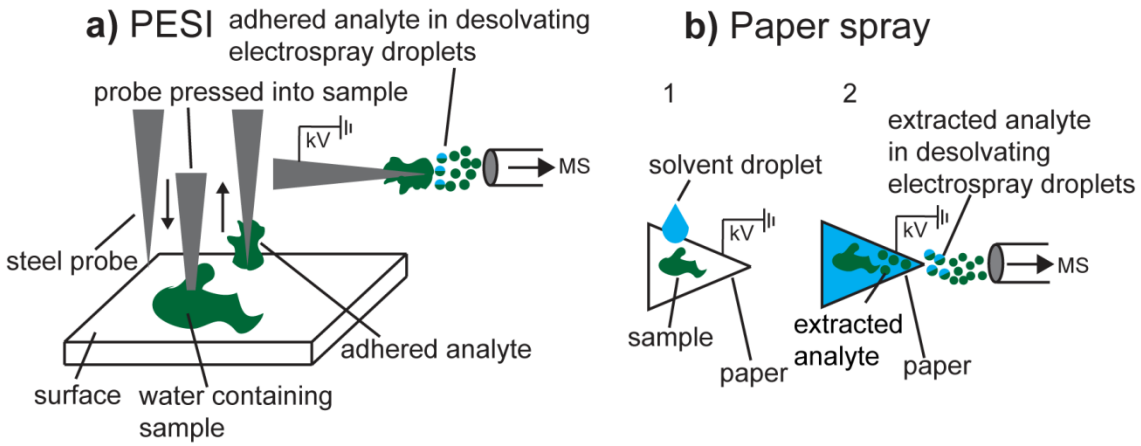
a) PESI
adhered analyte in desolvating electrospray droplets
probe pressed into sample
kV
MS
steel probe
adhered analyte
surface
water containing sample
b) Paper spray
1
2
extracted analyte in desolvating electrospray droplets
solvent droplet
kV
kV
MS
sample
paper
extracted analyte
paper

Tables

Table 1

Table 1 Lipid Classes Detected by MALDI and Corresponding Matrices.[a]

Lipid Class	Matrix	Sample	Reference
Phospholipids (pos)	CHCA	Tissue sections	[30]
	DAN	Tissue sections	[31]
	DHA	Tissue sections	[32]
	DHB	Standards, tissue sections, lipid extracts	[27, 33, 34]
	Di-FCCA	Lipid extracts	[35]
	Dithranol	Tissue sections	[36]
	Lumazine	Standards and lipid extracts	[49]
	MBT	Tissue sections, lipid extracts	[37, 38]
	PNA	Tissue sections, lipid extracts	[39, 40]
	THAP	Standards, tissue sections	[41]
Phospholipids (neg)	9-AA	Lipid extracts, egg chambers from a fly	[35, 42, 43]
	DAN	Tissue sections	[31]
	DHA	Tissue sections	[32, 44]
	DHB	Standards, lipid extracts	[33, 45]
	DMAN	Intact bacteria cells	[46]
	Lumazine	Standards and lipid extracts	[47]
	PNA	Lipid extracts, tissue sections	[39, 48, 49]
Sphingolipids/ Glycolipids	9-AA	Tissue sections, lipid extracts	[50-52]
	CHCA	Tissue sections, lipid extracts	[30, 53]
	DHB	Tissue sections, lipid extracts on TLC plate	[45, 54, 55]
	Dithranol	Tissue sections	[36]
	MBT	Lipid extracts	[37]
	THAP	Standards lipid extracts,	[41]
Glycerolipids	CHCA	Lipid extracts	[56]
	DHB	Standards, lipid extracts, single embryo and oocytes	[56-58]
	THAP	Lipid extracts	[41, 59]
Cholesterol	DHB[b]	Tissue sections, lipid extracts	[54, 60]
	Silver	Standards and cells	[61, 62]
Cholesterol Esters	DHB	Lipid extracts	[60, 63, 64]
Free fatty acids	DMAN	Standards, leaf material, fly body, blood	[65, 66]
	Graphene/ graphene oxide	Lipid standards, lipid extracts	[67]
	MTPFPP	Lipid extracts, saponified vegetable oil	[68, 69]
	Silver	Tissue sections	[70]
	TCNQ/Li	Lipid standards	[71]

[a] Note that this table is not intended as a comprehensive summary of all reported lipid-matrix combinations but rather highlights the variety of lipids that have been detected and the suitability of matrix compounds.

[b] Detected as the $[M+H-H_2O]^+$ ion.

9-AA, 9-aminoacridine; CHCA, α-cyano-4-hydroxycinnamic acid; DAN, 1,5-diaminonapthalene; DHA, 2,6-dihydroxyacetphenone; DHB, 2,5-dihydroxybenzoic acid; Di-FCCA, α-cyano-2,4-difluorocinnamic acid; DMAN, 1,8-bis(dimethylamino) naphthalene; MBT, 2-mercaptobenzothiazole; MTPFPP, *meso*-tetrakis (pentaflurophenyl) porphyrin; PNA, *p*-nitroaniline; TCNQ, 7,7,8,8-tetracyanoquinodimethane; THAP, 2,4,6-trihydroxyacetophenone.

Table 2

Table 2 Lipid classes detected from various surfaces by DESI-MS.

Lipid Class	Sample/Surface	Sub-Classes Detected (polarity)	Reference
Phospholipids (pos)	Tissue sections	PC, SM, PE, PS(+)	[185-188]
	PTFE (standards and extracts)	PC(+)	[182, 184]
	Glass (standards, extract, whole bacteria)	PC, SM, PE(+)	[182, 189, 190]
	TLC silica	PC, SM(+)	[184]
Phospholipids (neg)	Tissue sections	PS, PI, PE, PG(-)	[186, 188, 191, 192]
	PTFE (standards and extracts)	PC, PS, PE, PI(-)	[182, 184]
	Glass (standards, extract, whole bacteria)	PE, PG, PI(-)	[182, 189, 190]
	TLC silica	SM, PC, PI, PE, PS(-)	[183]
Sphingolipids (other than SM)	Tissue sections	Cer(+), LacCer(+), GalCer(+) ST(-)	[185, 186, 193]
	PTFE	ST(-)	[182]
	TLC Silica	LacCer(+), ST(-), GL(-)	[183, 184, 194]
Glycerolipids	Glass (olive oil)	TAG(+)	[195]
	Tissue sections	DAG(+), TAG(+)	[196, 197]
		DAG(-)	[198]
Cholesterol	Glass (standards, serum, cod liver oil)	(+)	[199]
	Tissue sections	(+)	[185, 199, 200]
Cholesterol Esters	Tissue sections	(+)	[201]
Fatty acids	Tissue sections	(-) (including eicosanoids)	[191, 192, 198]
	PTFE	(-)	[202]
	PTFE, paper	(+) (FFA, ethyl esters and prostaglandins)	[197]

Cer, ceramide; DAG, diacylglyceride; FFA, free fatty acid; GalCer, galactosylceramide; GL, ganglioside; LacCer, lactosylceramide; PC, phosphatidylcholine; PE, phosphatidylethanolamine; PG, phosphatidylglycerol; PI, phosphatidylinositol; PS, phosphatidylserine; PTFE, polytetrafluoroethylene; SM, sphingomyelin; ST, sulfatide; TLC, thin-layer chromatography.